A role of SUMOylation in proteostasis, centromere integrity and the DNA damage response

Liebelt, F.

CHAPTER 3

SUMOylation and the HSF1-regulated Chaperone Network Converge to Promote Proteostasis in Response to Heat Shock

Frauke Liebelt[1,3], Rebecca M. Sebastian[2,3], Christopher L. Moore[2], Monique P.C.Mulders[1], Huib Ovaa[1], Matthew D. Shoulders[2,4], Alfred C.O. Vertegaal[1,4]

[1]Department of Cell and Chemical Biology, Leiden University Medical Center, Leiden, RA 2300, The Netherlands,

[2]Department of Chemistry, Massachusetts Institute of Technology, Cambridge, MA 02139, United States

[3]These authors contributed equally; [4]These authors contributed equally

Published in *Cell Reports* in 2019

ABSTRACT

The role of stress-induced increases in SUMO2/3 conjugation during the heat shock response (HSR) has remained enigmatic. We investigated SUMO signal transduction at the proteomic and functional level during the HSR in cells depleted of proteostasis network com-ponents via chronic heat shock factor 1 inhibition. In the recovery phase post-heat shock, high SUMO2/3 conjugation was prolonged in cells lacking sufficient chaperones. Similar re-sults were obtained upon inhibiting HSP90, indicating that increased chaperone activity during the HSR is critical for recovery to normal SUMO2/3 levels post-HS. Proteasome inhibition likewise prolonged SUMO2/3 conjugation, indicating that stress-induced SUMO2/3 targets are subsequently degraded by the ubiquitin-proteasome system. Functionally, we suggest that SUMOylation can enhance solubility of target proteins upon HS, a phenomenon that we experimentally observe in vitro. Collectively, our results implicate SUMO2/3 as a rapid re-sponse factor that coordinates proteome degradation and assists the maintenance of proteo-stasis upon proteotoxic stress.

INTRODUCTION

The composition of the cellular proteome is dynamically matched to functional re-quirements via transcription, splicing, new protein synthesis, and protein turnover. Throughout this process, protein misfolding and aggregation are minimized by an extensive proteostasis network comprising chaperones, quality control mechanisms, and degradation pathways. The proteostasis network both facilitates productive folding and removes terminally misfolded or aggregated proteins[1,2].

Upon proteotoxic stress, the proteostasis network can become overloaded by excess misfolded proteins. Cellular responses like the heat shock response (HSR) are induced to resolve the misfolding and prevent the formation of toxic and/or insoluble protein aggregates. The HSR is coordinated by heat shock factors (HSFs) that induce the transcription of chaperones and quality control factors to resolve excessive protein misfolding[3]. HSF1 is the master regulator of the HSR. HSF1 is continuously expressed, and displays low basal activity sufficient only to maintain normal levels of cytosolic and nuclear proteostasis network components in the absence of proteotoxic stress. The majority of HSF1 under these conditions is maintained inactive in the cytoplasm in a monomeric form, apparently via binding to chaperones[4,5]. Increasing levels of misfolded proteins owing to either chronic proteotoxic stress (e.g., constitutive expression of a mutant, misfolding protein) or acute proteotoxic stress (e.g., HS or heavy metal oxidants) leads to chaperones being titrated off of HSF1 by interaction with the accumulating misfolding proteins, inducing HSF1 homotrimerization and translocation to the nucleus to initiate the extensive HSR transcriptional program[6]. Once the proteotoxic stress has been resolved, HSF1 is inactivated again via post-translational modifications or via binding to excess chaperones[7].

In addition to transcriptional remodeling, proteotoxic stress is known to rapidly but transiently induce high levels of specific protein post-translational modifications, including substantial increases in conjugation to ubiquitin (Ub), O-linked glycans, and small-ubiquitin related modifiers (SUMO)[8-13]. It is well-appreciated that Ub modification can enhance proteostasis in response to proteotoxic stress via promoting proteasomal degradation of misfolded proteins, and that O-glycosylation can inhibit the aggregation of at least certain intrinsically disordered proteins[14,15]. However, the role of dramatic increases in SUMO2/3 modification levels upon proteotoxic stress has remained enigmatic.

The SUMO family is a group of highly conserved proteins with a similar three-dimensional fold to Ub[16-18]. Like Ub, SUMO dynamically modifies lysine side chains on sub-strate proteins[19,20]. Three major isoforms (SUMO1, 2, and 3) are ubiquitously expressed in mammalian cells[16,21]. SUMO1 only shares 48% sequence identity with SUMO2 and SUMO3. SUMO2 and SUMO3 share the vast majority of their amino acid sequences (95% se-quence identity), cannot be distinguished by extant antibodies, and as such are often referred to collectively as SUMO2/3.

Shortly after the discovery of the SUMO2/3 family members, it was observed that these SUMO modifications rapidly accumulate upon HS, in contrast to SUMO1[10,21]. Proteomic analysis revealed increases in SUMO2/3 conjugation for a wide range of substrates[8,9,22]. Notably, SUMO2 is recruited to open chromatin during HS[23] and appears to be indispensable for full activation of the inducible HSPA1A (HSP70) gene[24]. Modification of HSF1 by both SUMO1 and SUMO2/3 is also induced during stress, and may modulate the transcription of heat shock proteins (HSPs) during later stages of stress[25,26]. Although stress-induced SUMOylation is widespread, the potential proteostatic functions and regulation of this

modification, which typically recovers to normal levels in a matter of 2–4 hrs after HS, are poorly understood.

We present evidence that the composition and activities of the cellular proteostasis network regulate SUMO2/3 dynamics during HS, and are critical determinants in the degra-dation of SUMOylated substrates by the ubiquitin-proteasome system. We further identify a unique subset of SUMOylated proteins that preferentially maintain SUMOylation for prolonged time periods during chronic proteostasis impairment. Finally, we present evidence that SUMOylation reduces the aggregation of substrate proteins *in vitro*. Our results implicate SUMOylation as a rapid response mechanism that is integrated within the chaperone and quality control networks, is essential for coordinating substrate degradation in response to proteotoxic stress, and may prevent substrate aggregation at least in certain cases. Considering the number of SUMOylated substrates associated with neurodegeneration and cancer[27,28], these findings lay the foundation for investigating the intersection of SUMO2/3 modifications with protein quality control systems in disease progression and severity.

RESULTS

Depletion of Proteostasis Factors via Chronic HSF1 Inhibition Delays Recovery of SUMO2/3 Conjugation Levels after Heat Shock

As SUMO2/3 conjugation is stimulated by a variety of stressors associated with protein misfolding, including heat and oxidative stress, we were first interested in determining whether an impaired protein folding environment sensitizing cells to proteotoxic stress would modulate stress-induced SUMOylation. To create an impaired proteostasis network, we globally depleted cytosolic and nuclear proteostasis factors by using chemical biology tools to regulate the activity of the master cytosolic proteostasis transcription factor HSF1. We previously showed that a doxycycline (Dox)-inducible, constitutively active dominant-negative variant of HSF1, termed dn-cHSF1 29, can inhibit the activity of endogenous HSF1 with high selectivity and potency (Figure 1A). Chronic expression of dn-cHSF1 results in reduced steady-state levels of key proteostasis network components, especially HSP40, HSP70, and HSP90 (Figure 1B; see also 29).

We examined the effects of this chaperone depletion on the dynamics of SUMO2/3 conjugation both during and after HS in HEK293T-REx cells. As expected, immediately post-HS a strong increase in SUMO2/3 conjugation was observed (Figure 1C). When HSF1 was not inhibited prior to HS, the rate of return to normal SUMO2/3 conjugation levels was rapid, with complete return to basal SUMOylation achieved within 2 hrs of recovery at 37 °C. In sharp contrast, chronic inhibition of HSF1 prior to HS delayed recovery of SUMO2/3 conjugation levels beyond 4 hrs during recovery at 37 °C (Figures 1C and S1A). Importantly, control experiments in HEK293T-REx cells expressing a Dox-inducible GFP construct did not show any Dox-mediated changes in SUMOylation dynamics (Figure S1B), confirming that the delayed recovery was due to the induction of dn-cHSF1. Metabolic activity after HS was not significantly reduced following chronic HSF1 inhibition (Figure S1C), indicating that cell growth was not influenced and that sustained SUMOylation could not be attributed to an overall impairment in cell health during HS recovery.

The difference in the recovery rates could not be attributed to either increases in basal SUMO2/3 conjugation, or to an increase in initial SUMOylation levels immediately following HS (Figures 1C and S1A). Instead, it was specifically the recovery to normal SUMO2/3 levels that was delayed by chronic HSF1 inhibition. Notably, these observations were not limited

to HEK293T-REx cells, as we observed a similar delay in recovery when HSF1 was chronically inhibited prior to HS in LX2 hepatic stellate cells (Figure S1D).

Chronic inhibition of HSF1 via Dox-induced expression of dn-cHSF1 not only basally depletes chaperones, but also prevents HSR induction upon HS. To distinguish between SUMO2/3 retention resulting from inhibition of the HS-induced HSR versus reduced basal proteostasis capacity prior to HS, we next sought to uncouple HSR inhibition from basal depletion of chaperones owing to chronic HSF1 inhibition by transiently inhibiting the HSR without significantly reducing basal expression of chaperones. Briefly, we expressed a genetic fusion of dn-cHSF1 conjugated to a destabilized variant of Escherichia coli dihydrofolate reductase (DHFR), which is rapidly degraded by the proteasome unless a stabilizing ligand (trimethoprim; TMP) is added to the cell culture media[29]. Using this system, we found that acute TMP treatment (4 hr) did not substantially impact basal chaperone expression (Figure 1D). However, HS-induced transcription of HSF1-mediated genes was substantially impaired (Figure S1E).

Using cells expressing the DHFR.dn-cHSF1 construct, we examined the dynamics of stress-responsive SUMO2/3 conjugation following acute (4 hr TMP) HS inhibition versus chronic (48 hr TMP) chaperone depletion prior to HS. Acute TMP treatment did not substantially alter either the accumulation of SUMO2/3 conjugates during HS or the rate of recovery (Figures 1D and 1E). In contrast, chronic inhibition of HSF1 using this TMP-regulated HSF1 construct fully recapitulated the consequences of Dox-inducible dn-cHSF1 expression (Figures 1D and 1E). Thus, alterations in stress-responsive SUMOylation dynamics are attributable to chronic HSF1 inhibition that engenders depletion of critical components within the proteostasis network and sensitizes the system to proteotoxic stress.

Proteomic Identification of SUMOylated Proteins Whose Recovery to Normal SUMO-Conjugation Levels post- Heat Shock is Delayed by Chronic HSF1 Inhibition

We next sought to identify the specific SUMOylation targets that preferentially retain SUMO2/3 when proteostasis capacity is reduced. To address this question, we used nickel-nitrilotriacetic acid (Ni-NTA) beads to purify SUMOylated proteins from HEK293T-REx cells co-expressing a His10-tagged SUMO2 along with Dox-inducible dn-cHSF1. Cells co-expressing a Dox-inducible GFP and His10-SUMO2 were used as a control for any effects of Dox treatment. Cells lacking the His10-SUMO2 construct were used as a control for non-specific binding to Ni-NTA beads.

We then used quantitative proteomics to study SUMO2 target protein dynamics be-fore, during, and after HS in basal and chronic HSF1 inhibition conditions (Figure 2A). Immunoblot analysis of the input samples prior to mass spectrometry analysis fully recapitulated our findings from Figure 1 (Figure 2B). In the proteomics, with a low stringency requiring only an average fold change ≥ 2, we identified 450 proteins that consistently showed increased SUMOylation immediately following HS. The extent of SUMO2 conjugation on 89% (n = 399) of these proteins returned to normal levels during the 4 hr recovery period in untreated cells. In contrast, recovery to normal SUMO2 levels was delayed for 77% (306) of the identified proteins when HSF1 was chronically inhibited (Table S1). We also observed striking enrichment of SUMOylated HSF1 immediately after HS and during recovery following Dox treatment, which can be attributed to a large extent to overexpression of dn-cHSF1 (Figure 2C). These observations demonstrate the vast influence of the proteostasis network on SUMOylated protein dynamics during HS recovery. Notably, we did not observe a global effect on the extent of SUMOylation immediately post-HS owing to chronic HSF1 inhibition.

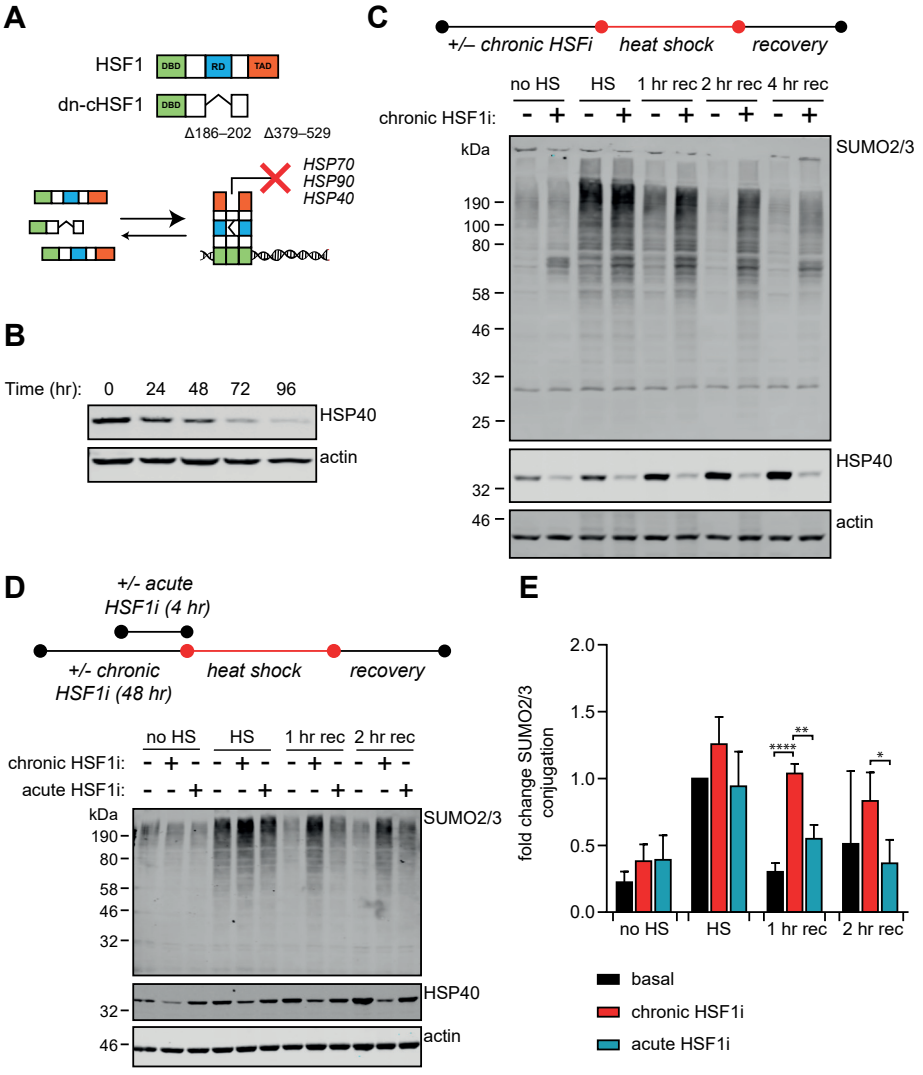

Figure 1. Depletion of Proteostasis Factors via Chronic HSF1 Inhibition Delays Recovery to Normal SUMO2/3 Conjugation Levels after Heat Shock. (**A**) Use of a dominant-negative, constitutively active HSF1 construct (dn-cHSF1), created via disruption of the regulatory domain (RD) by removing amino acids 186–202 combined with deletion of the transcription activation domain (TAD), for inhibition of endogenous HSF1. (**B**) Western blot analysis of HSP40 protein levels in response to different time periods of Dox-induced dn-cHSF1 induction in HEK293T-REx cells. (**C**) HEK293T-REx cells expressing Dox-inducible dn-cHSF1 were treated with Dox for 48 hrs (chronic HSF1i) prior to heat shock (HS). Cells were exposed to a HS at 43 °C for 75 min before returning to 37 °C for a recovery period (rec) and lysed as indicated. Total amounts of SUMOylated proteins were analyzed by immunoblotting. HSP40 levels were used to confirm induction of the heat shock response and functional HSF1 inhibition. (**D**) HEK293T-REx cells constitutively expressing DHFR.dn-cHSF1 were treated with trimethoprim (TMP) for 48 hrs (chronic HSF1 inhibition) or 4 hrs (acute HSF1 inhibition) prior to HS. Cells were subsequently exposed to HS and recovery as described in (A). Total amounts of SUMOylated proteins were determined by immunoblotting. (**E**) Quantification of total SUMO2/3 conjugation from (D) as compared to SUMOylation post-HS in basal proteostasis conditions. n = 3, error bars indicate standard deviation. Significance was determined using ANOVA analysis followed by post-hoc Tukey analysis, * = $p < 0.05$; ** = $p < 0.005$, **** = $p < 0.0001$.
See also Figure S1.

We also did not observe global changes in SUMOylation or SUMOylation dynamics as a result of Dox treatment in the Dox-inducible GFP control cells (Figures 2C and S2A, Table S1). We next set out to identify high-confidence proteins for validation and follow-up studies. We therefore adjusted our selection criteria to proteins having a ≥ 2-fold change as well as a p-value < 0.05 and identified 344 high-confidence SUMO2 target proteins that were significantly enriched immediately following HS, regardless of treatment condition (Tables S1 and S2). The extent of SUMO2 conjugation on 49% (n = 170) of these proteins returned to normal levels during the 4-hr recovery period in untreated cells (Table S3). Of this subset, recovery to normal SUMOylation levels was delayed for 42% (n = 72) of the identified proteins when HSF1 was chronically inhibited (Figure 2C and Table S4), as compared to vehicle treatment.

High-confidence SUMO2 conjugates whose recovery to basal SUMOylation levels was delayed by chronic HSF1 inhibition were enriched for DNA-associated factors, including proteins involved in transcription, recombination, and DNA repair (Figures 2D and S2B), consistent with the predominantly nuclear localization of SUMO. We further validated delayed SUMO2/3 recovery under conditions of chronic HSF1 inhibition for a number of the proteins identified in our mass spectrometry screen, engendering high confidence in our mass spectrometry results (Figure S3). Interestingly, we could also confirm a HSF1 inhibition-dependent effect on the SUMOylation dynamics of FoxM1 post-HS. FoxM1 is a protein that did not quite meet our strict filtering conditions for Figure 2C, indicating that such a stringent selection criteria can lead to false negatives. In combination with our low-stringency data analysis, these results further support the thesis that the proteostasis network is required to resolve a significant fraction of HS-induced SUMO2 targets.

Chronic HSF1 Inhibition Interferes with Degradation of SUMOylated and Ubiquitinated Proteins during Heat Shock Recovery

The clearance of SUMOylated proteins observed during HS recovery may occur ei-ther by removal of SUMO2/3 by the action of SUMO-specific proteases (SENPs) or by degradation of the SUMO2/3-conjugated proteins 30. Using a recently developed set of activity-based probes[31], we performed activity profiling of a set of endogenously expressed SENPs. The results indicated that proteostasis modulation by chronic HSF1 inhibition did not affect the activity of SENPs during HS or recovery (Figure S4).

We next sought to define if SUMOylated proteins were subjected to degradation during HS recovery. We first examined the effects of proteasome inhibition on SUMO2/3 conjugation during HS and recovery using two commercially available proteasome inhibitors, MG-132 and bortezomib. We observed that bortezomib did not induce basal SUMOylation at concentrations with comparable proteasome inhibitory activity as MG-132 (Figure S5A; note that bortezomib does not inhibit the β2 catalytic subunit of the proteasome, whereas MG-132 does inhibit this subunit[32]). We therefore chose to proceed with bortezomib to isolate HS and proteostasis-dependent impacts on degradation of SUMOylated proteins.

We found that proteasome inhibition using bortezomib delayed the recovery of global SUMO2/3 conjugates post-HS in a manner similar to the consequences of chronic HSF1 inhibition prior to HS. Indeed, either proteasome inhibition or chronic HSF1 inhibition resulted in SUMOylation remaining at > 80% of the levels of the maximal SUMOylation in vehicle-treated samples following a 2-hr recovery period. Notably, the effects of proteasome inhibition and chronic HSF1 inhibition on delaying SUMO2/3 recovery were partially additive, with SUMO2/3 conjugation remaining near 100% throughout the recovery period

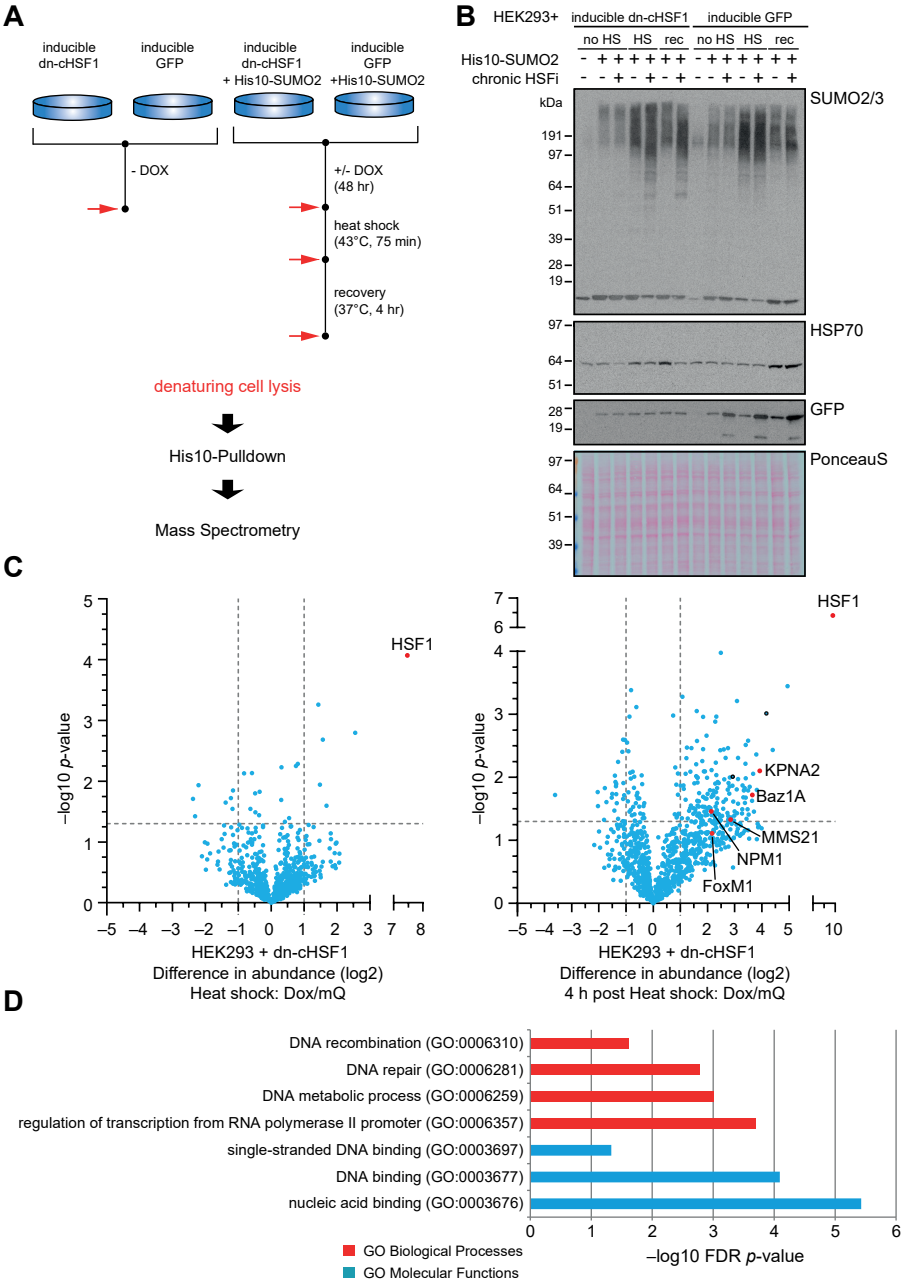

Figure 2. Proteomic Identification of SUMOylated Proteins Whose Recovery to Normal SUMO-conjugation Levels Post- Heat Shock is Delayed by Chronic HSF1 Inhibition. (**A**) Workflow for Figure 2. HEK293T-REx cells stably co-expressing His10-SUMO2 and either Dox-inducible dn-cHSF1 or Dox-inducible GFP were treated with Dox for 48 hrs (chron-ic HSF1 inhibition) prior to heat shock (HS). Cells were exposed to HS at 43 °C for 75 min before returning to 37 °C for a recovery period (rec). Red arrows indicate time points at which cells were lysed. SUMOylated proteins were purified by means of His10-pulldown, proteins were trypsinized, and peptides were analyzed by mass spectrometry. (**B**) Immunoblotting of cell lysates from (A) using antibodies against SUMO2/3, HSP70, and

when the treatments were applied in combination (Figures 3A, S5B, and S5C). Collectively, these observations suggest that a large fraction of SUMO2/3 conjugates are degraded by the proteasome in the recovery phase post-HS, indicating impaired degradation and, therefore, a stabilization of SUMO2/3 conjugates as a consequence of chronic HSF1 inhibition.

Because proteasomal degradation of proteins is regulated by ubiquitination, we next investigated Ub dynamics during HS recovery. Similar to SUMOylation dynamics, we observed an increase in Ub conjugates during HS that was rapidly reduced to pre-HS levels during the recovery period (Figure 3B). Chronic HSF1 inhibition prior to HS delayed recovery of Ub conjugation post-HS, although to a substantially lesser extent than for proteasome inhibition (Figures 3B and S5D). These results suggest that proteostasis factors, transcribed by HSF1, facilitate proteasomal degradation of ubiquitinated as well as SUMOylated substrates during HS recovery. As simultaneous inhibition of the proteasome and HSF1 resulted in a slight additive stabilization of SUMOylated proteins, but not of ubiquitinated proteins, we would not exclude an additional proteasome-independent pathway by which chaperones and other proteostasis factors stimulate a decrease in SUMOylation during recovery post-HS.

We next investigated if the identities of the ubiquitinated and SUMOylated substrates affected by chronic HSF1 inhibition coincided. Here, we examined Ub- and SUMO2- purified fractions for the presence and dynamics of specific proteins that we previously identified as showing delayed recovery to normal SUMO2 levels in Figure 2. The SUMOylation of the cell cycle regulator Forkhead box transcription factor FoxM1 was induced upon HS and decreased to pre-HS levels during recovery, but was stabilized by either proteasome inhibition or chronic HSF1 inhibition (Figure 3C). FoxM1 ubiquitination was also induced by HS and recovered post-HS in a proteasome and HSF1-dependent manner (Figure 3D). Additional SUMO2 substrates, identified by proteomics, showed similar SUMOylation and ubiquitination dynamics, indicating that both modifications were affected by chronic HSF1 inhibition on the same substrate proteins (Figures S5E and S5F).

Collectively, these data suggest that proteasomal degradation is a major, but not the exclusive, fate of SUMO2/3 and Ub conjugates during HS recovery. Chronic HSF1 inhibition interferes with this proteasomal degradation and therefore stabilizes ubiquitinated as well as SUMOylated subsets of the same target protein.

Chronic HSF1 Inhibition Selectively Impairs Degradation of SUMO2/3 and Ub co-modified Proteins during Heat Shock Recovery

SUMO and Ub both covalently attach to lysine residues in target proteins. The modifications are mutually exclusive at a specific modification site. However, SUMOylation and ubiquitination frequently co-exist at different sites on the same protein[33,34]. We observed in Figures 3C and 3D that FoxM1 was modified by both SUMO2/3 and Ub, and that the

< GFP. Total amounts of proteins in each lane were visualized by Ponceau S staining. (**C**) Volcano plots depicting statistical differences in abundance between proteins identified by mass spectrometry. Dashed lines indicate a cut-off at a *p* value ≤ 0.05 (–log10 *p* value ≤ 1.3) and a fold change of 2 (log2 = 1). Left panel shows SUMOylated proteins identified immediately post-HS in the Dox-inducible dn-cHSF1 cell line, specifically in the Dox-treated sample compared to the untreated sample. Right panel shows SUMOylated proteins identified 4 hrs post–HS in the Dox-inducible dn-cHSF1 cell line compared to the untreated sample. Proteins marked in red are either HSF1 or proteins that were further validated. (**D**) Selection of enriched gene ontology terms of biological processes and molecular functions for selected proteins that significantly retained SUMOylation 4 hrs post-HS when HSF1 activity was chronically inhibited.

See also Figures S2 and S3 and Tables S1, S2, S3, and S4.

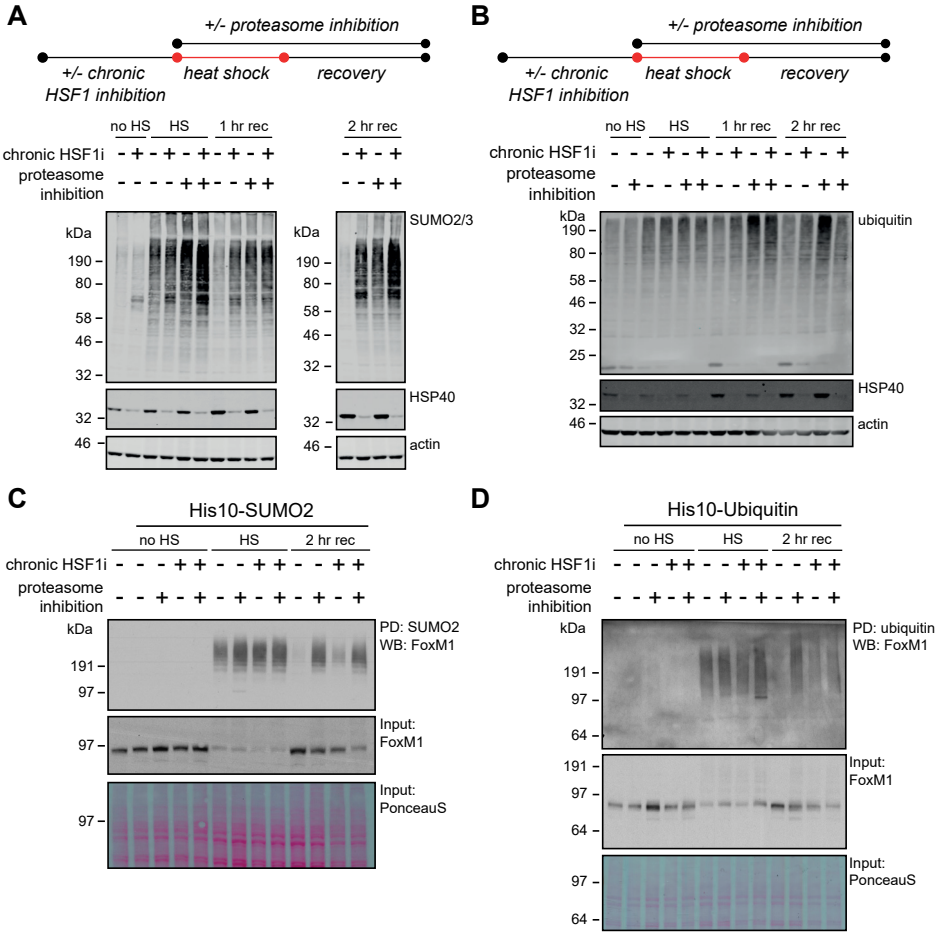

Figure 3. Chronic HSF1 Inhibition Interferes with Degradation of SUMOylated and Ubiquitinated Proteins during Heat Shock Recovery. (**A**) HEK293T-REx cells expressing Dox-inducible dn-cHSF1 were treated with Dox for 48 hr (chronic HSF1 inhibition), with 100 nM bortezomib (proteasome inhibition) immediately prior to heat shock (HS), or a combination of both. Cells were exposed to HS at 43 °C for 75 min before returning to 37 °C for a recovery period (rec) and lysed as indicated. Total amounts of SUMOylated proteins were analyzed by immunoblotting. HSP40 levels were used to confirm induction of the heat shock response and functional HSF1 inhibition. (**B**) HEK293T-REx cells expressing Dox-inducible dn-cHSF1 were treated as in (A). Total amounts of ubiquitinated proteins were analyzed by immunoblotting. (**C**) HEK293T-REx cells stably co-expressing His10-SUMO2 and Dox-inducible dn-cHSF1 were treated as in (A). SUMOylated proteins were purified by means of His10-purification. Elutions and inputs were analyzed by immunoblotting for FoxM1. Ponceau S stain was used as a loading control for inputs. (**D**) HEK293T-REx cells stably co-expressing His10-Ub and Dox-inducible dn-cHSF1 were treated as in (A). Ubiquitinated proteins were purified by means of His10-purification. Elutions and inputs were analyzed by immunoblotting for FoxM1. Ponceau S stain was used as a loading control for inputs. See also Figures S4 and S5.

dynamics of both modifications were influenced by chronic HSF1 inhibition. We therefore wondered if depletion of proteostasis network components by chronic HSF1 inhibition would preferentially impair degradation of the co-modified fraction of ubiquitinated or SUMOylated proteins.

We first examined the dynamics of ubiquitinated proteins in SUMO2 pulldowns and vice versa during either proteasome inhibition or chronic HSF1 inhibition. Within the SUMOylated

fraction, Ub was co-enriched upon HS, indicating an enrichment of co-modified proteins. The extent of Ub co-enrichment fell during HS recovery, but was enhanced by either chronic HSF1 inhibition or proteasome inhibition (Figure 4A). We observed the same dynamics for SUMO2/3 substrates within the Ub-purified proteins (Figure 4B). Collectively, these results support the conclusion that chaperone depletion interferes with the degradation of co-modified proteins during HS recovery.

We next wondered if the effect of chronic HSF1 inhibition was restricted to co-modified proteins, or if the stabilization of SUMO2/3 was merely a consequence of the stabilization of all ubiquitinated proteins. To answer this question, we investigated the ratio of SUMO2/3 in the pool of Ub-modified proteins. By inhibiting the proteasome, we expected to inhibit the degradation of all Ub-modified substrates, including co-modified proteins. If chronic HSF1 inhibition interfered mainly with the degradation of co-modified proteins, we would expect the ratio of SUMO2/3-modified to total Ub-modified proteins within the Ub-purified substrates to increase, as co-modified proteins would be stabilized whereas substrates modified by Ub alone would continue to be degraded. As shown in Figure 4C, we indeed observed a significant difference in SUMO/Ub ratio in the Ub-purified pool of proteins between proteasome inhibition and chronic HSF1 inhibition during the recovery post-HS, indicating a mechanism by which HSF1-induced factors selectively influence the degradation of co-modified proteins rather than all ubiquitinated proteins.

HSP90 Plays a Key Role in the Recovery to Normal SUMO2/3 Modification Levels following Heat Shock

As chronic HSF1 inhibition results in a reduction in proteostasis network capacity (Figure 1B), our data suggest that maintaining sufficient proteostasis capacity is critical for regulating the dynamics of SUMO2/3 and Ub substrates during HS recovery. We therefore sought to identify whether inhibition of specific proteostasis components would be sufficient to recapitulate the delayed recovery of SUMO2/3- and Ub-modified targets we initially observed with chronic HSF1 inhibition.

Using STA-9090 to inhibit HSP90, we examined the dynamics of SUMO2/3 and Ub conjugates following HS. We found that HSP90 inhibition, like chronic HSF1 inhibition, resulted in delayed recovery of > 50% of SUMO2/3 conjugates following a 2-hr recovery period (Figures 5A, 5B, and S6A). Similarly, we observed a delayed recovery post-HS of total ubiquitination upon HSP90 inhibition (Figures S6B and S6C). To investigate if HSP90 inhibition affects the same SUMOylated substrates we previously identified using proteomics (Figure 2), we purified SUMO2 conjugates and Ub conjugates and examined the dynamics of target proteins upon HS following either chaperone depletion or HSP90 inhibition. Indeed, we observed a HSF1- and HSP90-dependent decrease of FoxM1 SUMOylation and ubiquitination during the recovery period (Figures 5C and 5E). Similar effects were observed for other proteins (Figures S6D and S6E). HSP90 inhibition also prolonged retention of co-modified proteins, as observed for SUMO2/3 co-modified proteins in the Ub pulldowns and vice versa (Figures 5D, 5F, and S6F), and led to an increase in SUMO2/3 relative to Ub within Ub-purified proteins (Figure S6F).

Collectively, these data indicate that HSP90 inhibition alone can at least partially recapitulate the effects of chronic HSF1 inhibition, delaying the recovery of SUMOylated and Ub co-modified substrates post-HS. These observations suggest that HSP90 is a key chaperone effector that promotes the degradation of co-modified proteins.

SUMOylation of Substrate Proteins Enhances Solubility

A key role of Ub on the co-modified proteins appears to be efficient proteasome delivery and processing of the target protein. In contrast, the role of SUMO is less clear. We noted that SUMO has been used extensively as a solubility tag to prevent inclusion body formation during protein expression in *Escherichia coli*[35,36] and is also proposed to modulate aggregation of proteins associated with neurodegenerative disorders[28,37]. Therefore, we next used an *in vitro* assay to explore the possibility that rapid SUMO2/3 conjugation could act as a solubility tag on target proteins identified from our proteomic studies. Solubility enhancement mediated by SUMOylation could prevent aggregation of terminally misfolded proteins prior to their clearance by proteasomal degradation, a process that could be facilitated by chaperones during HS recovery.

To address this possibility, we investigated the aggregation behavior of selected SUMO-tagged proteins identified from our proteomics screen in Figure 2, using *in vitro* thermal shift assays. MMS21 was expressed in *E. coli* with or without an N-terminal SUMO3 tag, and the isolated protein was analyzed by a thermal shift assay to determine the aggregation temperature (T_{agg})[38]. We observed that the Tagg of N-SUMO3-MMS21 was ~7 °C higher than that of untagged MMS21 (Figure 6A).

This intriguing result, obtained using a non-natural N-terminal fusion of a single SUMO3 moiety to MMS21, prompted us to then further investigate a more biologically realistic situation. Given that proteins from the proteomics screen were often conjugated to multiple SUMO2/3 moieties, we explored the impact of multiple SUMO2/3 modifications on FoxM1 using *in vitro* SUMOylation. Similar to MMS21, conjugation of SUMO2/3 protected FoxM1 against heat-induced aggregation (Figure 6B). Furthermore, increasing SUMOylation appeared to stabilize FoxM1 additively, with higher order SUMO2/3 conjugates showing almost no aggregation at temperatures up to 70 °C. The presence of unmodified FoxM1 was also prolonged in the soluble fraction when SUMOylated proteins were present, indicating that the presence of SUMOylated proteins could even have a beneficial effect on the solubility of non-SUMOylated proteins in the vicinity (Figure 6B). We further investigated the impact of SUMOylation on FoxM1 during extended HS at moderate temperatures identical to the temperatures used in cellular studies. While unmodified FoxM1 demonstrated progressive aggregation at 43 °C, highly SUMOylated FoxM1 remained soluble throughout the duration of HS (Figure 6C). These results suggest that SUMO alters biophysical properties of the target protein and thereby decreases aggregation propensity. In cells, a likely consequence would be the promotion of proteasomal clearance during HS recovery by preventing the formation of otherwise insoluble and potentially irreversible aggregates.

DISCUSSION

The dynamic nature of protein post-translational modifications makes them particularly well-suited to regulate cellular processes during stress responses, as they can act rapidly in response to stimuli and their reversible nature makes them suitable to act in a transient manner. Here, we have explored the enigmatic role of SUMO signaling in the HSR and identified a unique subset of HS induced SUMO2/3 targets preferentially regulated by the proteostasis network.

The precise mechanism for enhanced SUMOylation upon heat stress remains to be investigated in detail. Pinto and co-workers have shown that heat stress inactivates SUMO proteases[39]. Our data recapitulate this observation, as we observe the inactivation of SENP1

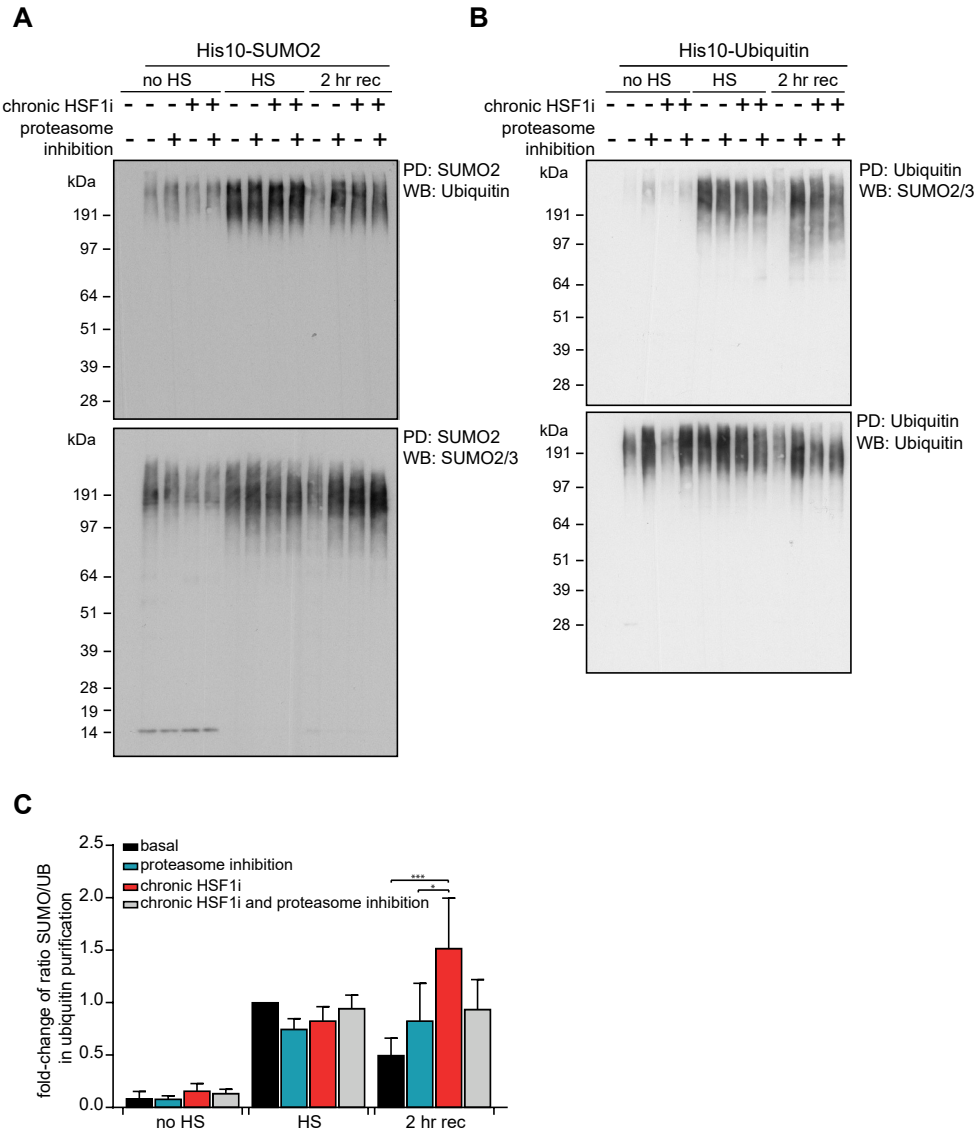

Figure 4. Chronic HSF1 inhibition selectively impairs degradation of SUMO2/3 and Ub co-modified proteins during heat shock recovery. (**A**) HEK293T-REx cells stably co-expressing His10-SUMO2 and Dox-inducible dn-cHSF1 were treated with Dox for 48 hrs (chronic HSF1i) prior to heat shock (HS), with 100 nM bortezomib (proteasome inhibition) immediately prior to HS, or a combination of both. Cells were exposed to a HS at 43 °C for 75 min before returning to 37 °C for a recovery period (rec) and lysing as indicated. Elutions were analyzed by immunoblotting for Ub and SU-MO2/3. (**B**) HEK293T-REx cells stably co-expressing His10-Ub and Dox-inducible dn-cHSF1 were treated as in (A). Elutions were analyzed by immunoblotting for SUMO2/3 and Ub. (**C**) Quantification of (B). Graph shows fold change of the ratio of SUMOylated proteins over ubiquitinated proteins in His10-Ub purified elutions as compared to the ratio after HS under basal proteostasis conditions. n = 3, error bars represent SD. Significance was determined using ANOVA followed by post-hoc Tukey's multiple comparison test, * = $p < 0.05$; *** = $p < 0.001$.

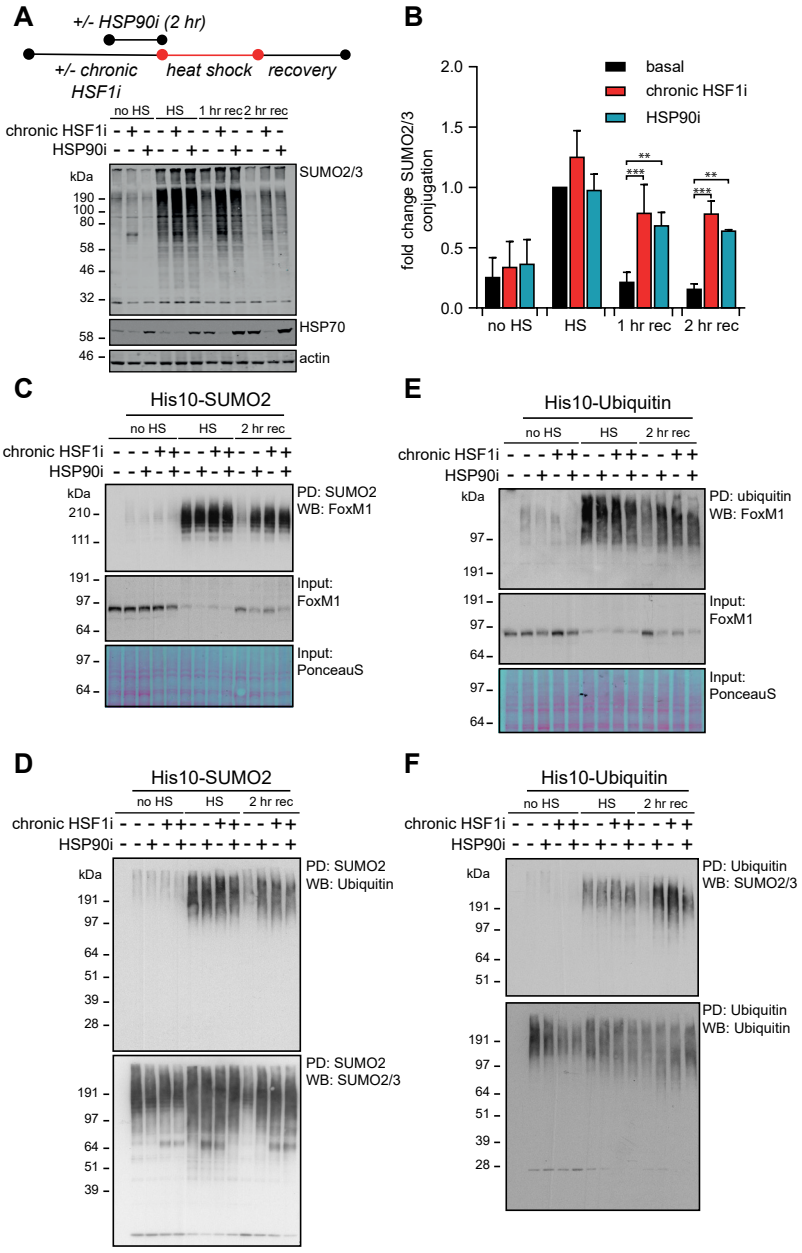

Figure 5. HSP90 Plays a Key Role in the Recovery of SUMO2/3 Modification Following Heat Shock. (**A**) HEK293T-REx cells expressing Dox-inducible dn-cHSF1 were either treated with Dox for 48 hrs (chronic HSF1 inhibition) prior to heat shock (HS), with 500 nM STA-9090 (HSP90i) 2 hrs prior to HS, or with a combination of both. Cells were exposed to a HS at 43 °C for 75 min before returning to 37 °C for a recovery period (rec) and lysed as indicated. Total amounts of SUMOylated proteins were analyzed by immunoblotting. HSP70 levels were used to confirm induction of the heat shock response and functional HSF1 inhibition. (**B**) Quantification of fold-change of SUMOylation from (A) as compared to SUMOylation after HS under the basal proteostasis conditions. n = 3, error bars indicate standard deviation. Significance was determined using ANOVA analysis followed by post-hoc Tukey analysis, * = $p < 0.05$; *** = < 0.0005. (**C**) HEK293T-REx cells stably co-expressing His10-SUMO2 and Dox-inducible dn-cHSF1 were

and SENP3 in response to heat stress (Figure S4B). Whether prolonged inactivation of SUMO proteases is responsible for prolonged increases of SUMOylation upon heat stress combined with chronic HSF1 inhibition is less clear, as our data did not convincingly show an HSF1-dependent inactivation of SENPs (Figure S4B). Alternatively, prolonged increases in activity of the SUMO conjugation machinery could explain prolonged increases of SUMOylation upon heat stress combined with chronic HSF1 inhibition. If this is the case, then we would expect higher auto-SUMOylation activity of SUMO E3 ligases[40]. SUMOylation of PIAS family members PIAS4 and MMS21 did increase in response to chronic HSF1 inhibition, as shown by mass spectrometry. We confirmed this result for MMS21 by immunoblotting (Figure S3A). We therefore expect that PIAS4 and MMS21 could mechanistically contribute to enhanced SUMOylation upon chronic HSF1 inhibition.

Conjugation of SUMO2/3 May Act as an Early Responder to Misfolded Proteins during Heat Shock

The key function of the transcription factor HSF1 is to activate genes encoding chap-erones and other proteostasis factors required to address protein misfolding induced by increased temperature or other stressors[41]. The transcriptional nature of this response results in a time gap between the rapid onset of proteotoxic stress and the availability of sufficient amounts of new chaperones to address the misfolded proteins[42]. Given that SUMOylation accumulates rapidly after onset of HS, and the extensive use of SUMO as a linear fusion to recombinant proteins to enhance solubility[43,44], we hypothesized that SUMOylation could potentially be functioning to deter aggregation during early stages of HS.

We explored the effect of SUMOylation on the solubility of target proteins upon HS *in vitro* and established that SUMOylation can have a profoundly solubilizing effect on its target proteins. Given the low substrate occupancy of SUMO2/3 on target proteins, it is unlikely that SUMOylation *in vivo* globally shifts the aggregation propensity of the total pool for its targets. Rather, these data suggest that SUMOylation may function to survey and tag unfolded proteins at particular risk for aggregation and facilitate their degradation through subsequent ubiquitination and proteasomal degradation. N-Linked glycosylation in the endoplasmic reticulum is also known to enhance solubility and facilitate interactions with protein folding machinery[45], suggesting that cells commonly utilize post-translational modifications to support proteostasis during stress conditions. These results therefore provide a possible method for cells to address the time-gap between stress onset and increased chaperone levels by acting as an early-response factor that can act rapidly to keep unfolded proteins soluble and prevent their accumulation into insoluble aggregates.

Mechanistically, it has been shown previously that the SUMO conjugation machinery recognizes disordered regions in target proteins[46]. As proteins that are unfolded will display increased levels of disordered regions, direct recognition of these regions by the SUMO conjugation machinery may provide a mechanism for this machinery to focus on unfolded target proteins. Under normal proteostasis conditions, SUMO mostly targets lysines which are located in a SUMOylation consensus motif (ψKxE, where ψ is a large hydrophobic amino

<treated as in (A) with a 2 hr recovery at 37 °C. SUMOylated proteins were purified by means of His10-purification. Elutions and inputs were analyzed by immunoblotting for FoxM1. Ponceau S stain was used as a loading control for inputs. (**D**) As for (C). Elutions were analyzed by immunoblotting for Ub and SUMO2/3. (E) HEK293T-REx cells stably co-expressing His10-Ub and Dox-inducible dn-cHSF1 were treated as in (A) with a 2 hrs recovery at 37 °C. Ubiquitinated proteins were purified by means of His10-purification. Elutions and inputs were analyzed by immunoblotting for FoxM1. Ponceau S stain was used as a loading control for inputs. (**F**) As for (E). Elutions were analyzed by immunoblotting for SUMO2/3 and Ub. See also Figure S6.

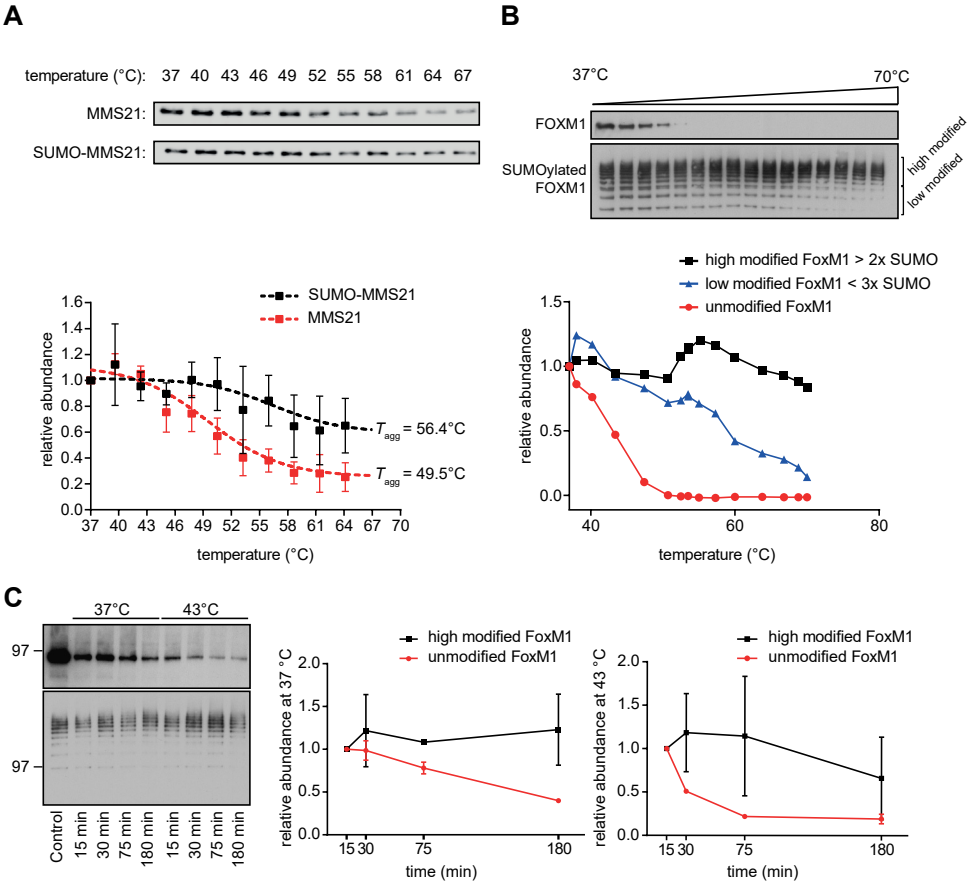

Figure 6. SUMOylation of Substrate Proteins Enhances Solubility. (**A**) Recombinant MMS21 fused to SUMO3 was exposed to increasing temperatures (37–67 °C). Soluble fractions were isolated from temperature-induced aggregates by centrifugation and analyzed by immunoblotting with a specific antibody against MMS21. The plot shows relative fold change of soluble MMS21 normalized to the soluble MMS21 at 37 °C, n = 3, error bars represent standard deviation. Data were fit to a sigmoidal curve in Prism to determine aggregation temperature (T_{agg}). (**B**) Recombinant FoxM1 was expressed and in vitro SUMOylated in E. coli, and in-vitro thermal shift performed as in (A). The soluble fraction of non-modified and SUMOylated FoxM1 was then analyzed by immunoblotting for FoxM1. The plots show relative fold-change of FoxM1 in the soluble fraction, comparing the highly SUMOylated FoxM1 species (>FoxM1-3x SUMO), modestly SUMOylated FoxM1 species (<FoxM1-3x SUMO) and un-modified FoxM1. (**C**) Recombinant FoxM1 was expressed and in vitro SUMOylated in E. coli, subsequently purified and incubated at either 37 °C or 43 °C for 15, 30, 75 min or 180 min. The soluble fraction of non-modified and SUMOylated FoxM1 was then analyzed by immunoblotting for FoxM1. The plots show relative fold change of FoxM1 in the soluble fraction comparing the highly SUMOylated FoxM1 species (>FoxM1-3x SUMO) to unmodified FoxM1 in two biological replicates.

acid). SUMOylation was reported to become more promiscuous during HS, targeting lysines that are not located in the consensus motif and demonstrating the possibility of a more general protective purpose for SUMOylation during HS[22].

Our results indicate that both SUMO2/3 and Ub are involved in the HSR. Whereas Ub has been named after its 'ubiquitous' cellular levels[47], SUMO has previously been consid-ered to be a low abundance protein[48]. Our data thus pose the challenge as to why a low abundance protein modifier would be used to deal with extensive protein misfolding. Proteomics

methods have been developed that can determine the copy numbers of proteins in cells[49]. The authors have shown that Ub is indeed one of the most abundant cellular proteins, with over 14 million copies per cell, ranking as the 10th most abundant cellular protein. Intriguingly, they found nearly 9 million copies of SUMO2 per cell, ranking SUMO2 as the 20st most abundant cellular protein. Thus, the difference in overall copy number per cell between Ub and SUMO2 is small. Additionally, given that Ub is present throughout the cell whereas SUMO2 is predominantly located in the nucleus, nuclear SUMO2 and Ub levels are expected to be rather similar. Therefore, SUMO2 should also be considered to be an abundant protein, making it a suitable early-response factor.

Despite the high abundance of SUMO and global SUMO conjugation within the nucleus, especially after HS, only a small fraction of a specific protein pool is targeted for SUMOylation. Whereas the SUMO- and ubiquitin-modified versions of target proteins are degraded by the proteasome, we did not observe that proteasomal inhibition affected the total pool of these targets, due to the substoichiometric nature of the modifications. We did, however, observe a clear stabilization of the SUMOylated and ubiquitinated version of selected targets in our bortezomib experiments (Figure 3 and S5). This finding is in line with earlier observations in the ubiquitin field indicating that the ubiquitiated portion of many proteins increased in response to proteasomal inhibition without noticeable changes in total levels of these proteins[50].

Because SUMO modifications are not known to directly target proteins to the proteasome for degradation, we consider it likely that subsequent ubiquitination is required for target protein degradation. Therefore, early conjugation of SUMO2/3 and subsequent ubiquitination works in concert to likely minimize aggregation of misfolded proteins by ensuring solubility and also by promoting degradation, respectively (Figure 7).

Proteostasis Factors facilitate Proteasomal Degradation of Co-modified Proteins

In the absence of HSF1, prolonged retention of SUMO2/3 during HS recovery indicates that proteostasis factors are required to resolve irreversible folding problems. Although SUMO2/3 might be able to act as an early-response factor to prevent aggregation of misfolded proteins, this action is apparently insufficient for refolding of the majority of proteins involved. Dissolution of misfolded proteins can either be carried out via refolding of the misfolded proteins, or via degradation by the ubiquitin-proteasome system. The pronounced effects of proteasome inhibition on overall SUMO2/3 conjugate levels during HS recovery indicates that a majority of SUMO2/3 targets are degraded. Refolding of SUMOylated misfolded proteins by the chaperones thus appears to not be very successful. Nevertheless, chaperones, especially HSP90, appear to be needed to facilitate the proteasomal degradation of misfolded proteins. Whether this degradation is mediated by HSP90 directly via either shuttling co-modified proteins to the proteasome or an effect of HSP90 on the activity of the proteasome itself remains to be resolved. Both scenarios seem possible, as chaperones have been identified as proteasome-interacting factors[51]. Of note, chaperones are predominantly located in the cytoplasm, indicating limited availability of chaperones for the regulation of nuclear proteins. In contrast, SUMO2/3 are predominantly located in the nucleus and could therefore potentially compensate for the limited availability of chaperones in the nucleus at the early phase of the HSR.

Chaperone-dependent degradation or refolding both prevent the formation of protein aggregates that are linked to many diseases, including aging-related neurodegeneration[52,53]. Once aggregates have formed, they appear to be resistant to protein degradation and pos-

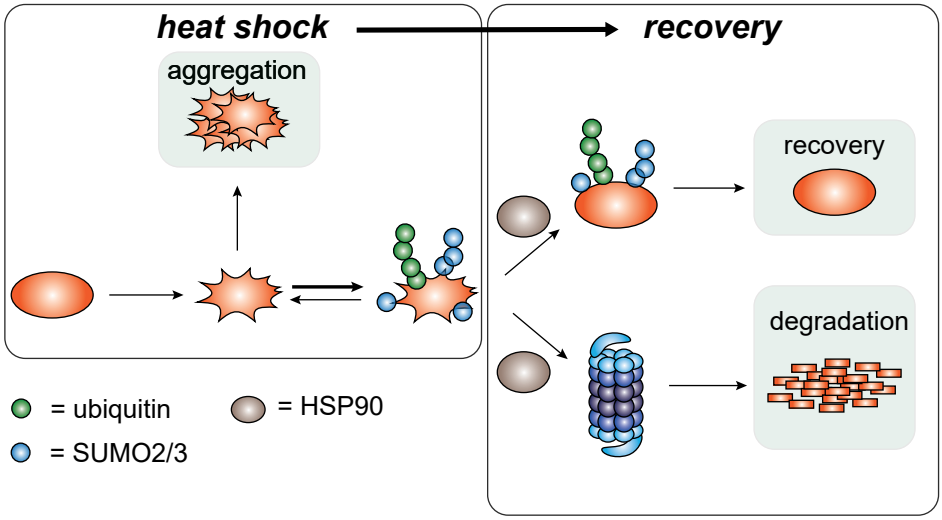

Figure 7. SUMO2/3 plays a Key Role as an Integrated Component of the Proteotoxic Stress Response.
Upon HS, a transient increase in SUMO2/3 conjugation to target proteins is observed, which may function in part to prevent irreversible aggregation of target proteins (reduced aggregation was demonstrated in vitro). SUMO2/3 modified proteins are frequently co-modified by Ub, and a large fraction of these co-modified proteins are subsequently degraded by the proteasome during HS recovery in a chaperone-dependent manner.

sess a high propensity to self-propagate and accrue in inclusion bodies [54]. Interestingly, SUMO has been found in disease-associated protein aggregates[55], suggesting a possible role in responding to or modifying aggregation-prone proteins. Our findings demonstrate clear con-nections between a functional proteostasis network and the post-translational modifications of Ub and SUMO2/3. Further improving our understanding of these connections might aid the development of treatment strategies for diseases characterized by the accumulation of toxic protein aggregates.

ACKNOWLEDGEMENTS
We thank Dr. R. González-Prieto for assistance with mass spectrometry. The laboratory of A.C.O.V. is supported by the European Research Council (ERC) and the Netherlands Organisation for Scientific Research (NWO). This work was also supported by the National Institute on Aging of the NIH Grant 5R21AG054961 to M.D.S and by the National Institute of Environmental Health Sciences of the NIH under award P30-ES002109. C.L.M. was supported by an NSF Graduate Research Fellowship. The mass spectrometry proteomics data have been deposited to the ProteomeXchange Consortium via the PRIDE partner repository with the dataset identifier PXD010231.

AUTHOR CONTRIBUTIONS
A.C.O.V. and M.D.S. conceived the project. F.L., R.M.S., C.L.M., A.C.O.V. and M.D.S. designed experiments. F.L., R.M.S., and C.L.M. conducted experiments. M.P.C.M. and H.O. provided key reagents. F.L., R.M.S., A.C.O.V., and M.D.S. drafted the manuscript. All authors analyzed data and edited the manuscript.

DECLARATION OF INTERESTS

H.O. is founder and a shareholder of UbiqBio B.V., a company that markets research reagents. All other authors declare no competing interests.

SUPPLEMENTARY DATA

Supplementary data tables can be found online

Key Recource Table

REAGENT or RESOURCE	SOURCE	IDENTIFIER
Antibodies		
SUMO2/3 mouse monoclonal	Abcam	Cat# ab81371; RRID:AB_1658424
SUMO2/3 mouse monoclonal	University of Iowa	8A2
HSP40 rabbit polyclonal	Enzo	Cat# ADI-SPA-400; RRID:AB_10631418
HSP70 rabbit polyclonal	Enzo	Cat# ADI-SPA-811D; RRID:AB_2621431
β-Actin mouse monoclonal	Sigma	Cat# A1978; RRID:AB_476692
ACF1/Baz1A rabbit polyclonal	Bethyl Laboratories	Cat# A301-318A-T; RRID:AB_937730
RCH1/KPNA2 rabbit polyclonal	Bethyl Laboratories	Cat# A300-483A-T; RRID:AB_451018
MMS21 rabbit polyclonal	Bethyl Laboratories	Cat# A300-129A; RRID:AB_2142840
NPM 1 rabbit polyclonal	Bethyl Laboratories	Cat# A302-402A; RRID:AB_1907285
SENP1 rabbit monoclonal	Abcam	Cat# ab108981; RRID:AB_10862449
SENP3 rabbit monoclonal	Cell Signaling Techol-ogy	Cat# 5591P; RRID:AB_10695540
SETDB1 rabbit monoclonal	Cell Signaling Techol-ogy	Cat# 2196S; RRID:AB_823637
SENP6 mouse monoclonal	Sigma	Cat # WHP0026054M1; RRID:AB_1843525
FoxM1	Santa Cruz	Cat# sc-502; RRID:AB_631523
Ubiquitin Mouse monoclonal	Millipore	Cat# 04-263; RRID:AB_612093
Ubiquitin	Santa Cruz	Cat# sc-8017; RRID:AB_628423
Bacterial and Virus Strains		
BL21(DE3)	New England BioLabs	Cat# C2527I
Chemicals, Peptides, and Recombinant Proteins		
STA-9090	MedChem Express	Cat# HY-15205
Doxycyline	Alfa Aesar	Cat# J63805
Trimethoprim	Matrix	Cat# 058373
Bortezomib	ChemGood	Cat# C-1279
MG-132	Fischer Scientific	Cat# NC9326288
Resazurin Sodium Salt	Sigma	Cat# R7017-5G
Rho-SUMO2-PA	31	NA
K11 di-SUMO VA ABP	31	NA
Critical Commercial Assays		
4–12% BoltTM Bis–Tris	ThermoFisher	NW04125BOX
NuPageTM 3–8% Tris-acetate	ThermoFisher	EA03755BOX
EZNA Total RNA Kit I	Omega	Cat# R6834-02
High-Capacity cDNA Reverse Transcription Kit	Applied Biosystems	Cat# 4368814
Fast Start Universal SYBR Green Master Mix	Roche	Cat# 4913850001
Deposited Data		

ProteomeXchange (via PRIDE database)	This paper	PXD010231
Experimental Models: Cell Lines		
Human: HEK293T-REx	Life Technologies	Cat# R71007
Human: LX2	EMD Millipore	Cat# SCC064; RRID:CVCL_5792
Recombinant DNA		
pET-15b	Novagen	Cat# 69661
pET11a-SUMO3	56	Addgene Plasmid #53143
pDEST17	Invitrogen	Cat# 11803012
pT-E1E2S2	57	NA
Lentiviral His10-SUMO2 IRES GFP	58	NA
Lentiviral His10-Ubiquitin IRES Puro	34	NA
pLenti CMV/TO Zeo dn-cHSF1	29	NA
pLenti CMV/TO Zeo GFP	29	NA
pLenti CMV Puro DHFR.dn-cHSF1	29	NA
Software and Algorithms		
MaxQuant ver 1.5.6.0	Max Planck Institute	http://www.biochem.mpg.de/5111795/maxquant
Perseus ver 1.5.6	Max Planck Institute	http://www.biochem.mpg.de/5111810/perseus
PANTHER	Gene Ontology Consortium	http://pantherdb.org/
Image Studio Lite ver 5.2	Li-COR	https://www.licor.com/bio/products/software/
GraphPad Prism 7	GraphPad	https://www.graphpad.com
ImageJ	Fiji	https://imagej.net/Welcome
Other		
Triple-disc C18 reverse phase stage-tips	59	NA

Contact For Reagent And Resource Sharing
Further information and requests for resources and reagents should be directed to and will be fulfilled by the Lead Contact, Matthew D. Shoulders (mshoulde@mit.edu).

Experimental Model And Subject Details
Human cell lines HEK293T-REx cells (human embryonic kidney, female) and LX2 cells (human hepatic stellate, male) were cultured at 37 °C in DMEM supplemented with 10% FBS and 1% penicillin/streptomycin/glutamine in a 5% CO2 atmosphere.
Environmental Stress Conditions: All heat shock experiments were performed at 43 °C and 5% CO2 for 75 min. For the recovery post-heat shock, cells were kept at 37 °C and 5% CO2 for the indicated time periods.

METHOD DETAILS

Lentivirus
Stable HEK293T-REx cells containing the Dox-inducible dn-cHSF1 and constitutively expressing FKBP.cHSF1 were prepared as previously described[29]. Lentiviruses encoding His10-SUMO2-WT-IRES-GFP[58] or His10-ubiquitin-WT-IRES-puro were transduced with an MOI (multiplicity of infection) of 3 using the third-generation lentiviral system into the previously generated HEK293T-REx cells containing both FKBP.cHSF1 and Dox-inducible dn-cHSF1 29. His10-SUMO2-WT-IRES-GFP expressing cells were sorted by fluorescence-aided cell sorting (FACS) on the BD FACSAriaIIITM cell sorter for low GFP expression to limit His10-SUMO2 expression. His10-ubiquitin-WT-IRES-PURO expressing cells were selected by supplementing the cell medium with 1μg/ml puromycin.

Immunoblotting Analysis
Cells were lysed in SNTBS buffer consisting of 2% SDS, 1% N-P40, 50 mM TRIS at pH 7.5, and 150 mM NaCl for whole lysate analysis of HEK293T-REx and LX2 cells. Proteins were separated by a 4–10% SDS-PAGE gel then transferred to a nitrocellulose membrane. Pulldown elutions and inputs were separated on either 4–12% BoltTM Bis-Tris or NuPageTM 3–8% Tris-acetate (anti-Baz1A) gradient gels. Following a 30 min blocking step in 5% milk, blots were incubated overnight with the appropriate primary antibodies and for 1 hr with the appropriate 680 or 800 nm fluorophore labeled secondary antibodies from Li-COR Biosciences or HRP-conjugated goat anti-mouse IgG, HRP-conjugated donkey anti-rabbit IgG from Pierce. Detection was performed on a Li-COR Biosciences Odyssey Imager for fluorophore-coupled secondary antibodies and with PierceTM ECL Plus Western Blotting substrate for HRP-coupled secondary antibodies. Band quantification was performed in Image Studio Lite or ImageJ (Fiji).

Quantitative RT-PCR.
The relative mRNA expression levels of selected heat shock re-sponse genes were measured using quantitative RT-PCR. HEK293T-REx cells expressing DHFR.dn-cHSF1 were treated with 10 μM TMP for 0, 2, 4, or 8 hr prior to challenge with a heat shock at 43 °C for 75 min. RNA was extracted using the EZNA Total RNA Kit I (Omega). qRT-PCR reactions were performed on cDNA prepared from 1000 ng of total cellular RNA using the High-Capacity cDNA Reverse Transcription Kit (Applied Biosystems). The Fast Start Universal SYBR Green Master Mix (Roche) and appropriate primers purchased

Sigma were used for amplifications (6 min at 95 °C then 45 cycles of 10 s at 95 °C, 30 s at 60 °C) in a Light Cycler 480 II Real-Time PCR machine. The primers used for DNAJB1 were 5′-TGTGTGGCTGCACAGTGAAC-3′ (forward) and 5′-ACGTTTCTCGGGTGTTTTGG-3′ (reverse), primers for HSPA1A were 5′-GGAGGCGGAGAAGTACA-3′ (forward) and 5′-GCTGATGATGGGGTTACA-3′(reverse), primers for HSP90AA1 were 5′-GATAAACCCTGACCATTCC-3′ (forward) and 5′-AAGACAGGAGCGCAGTTTCATAAA-3′ (reverse) and primers for RPLP2 5′-CCATTCAGCTCACTGATAACCTTG-3′ (forward) and 5′-CGTCGCCTCCTACCTGCT-3′ (reverse). Transcripts were normalized to the housekeep-ing genes RPLP2 and all measurements were performed at least in triplicate. Data were analyzed using the LightCycler® 480 Software, Version 1.5 (Roche) and data are reported as the mean ±95% confidence intervals.

Resazurin Assay.

HEK293T-REx cells expressing dn-cHSF1 were plated at 5,000 cells/well in a 96-well black bottom plate. Cells were subsequently treated with either Dox or DMSO for 48 hr prior to HS. Cells were exposed to HS at 43 °C for 75 min before returning to 37 °C for recovery. At the indicated time points post recovery, 15.00 µl of a 0.10 mg/mL solution of resazurin (sodium salt) was added to wells. Reduction of resazurin was monitored by fluorescence on a Gen5 plate reader (λ_{ex}: 530, λ_{em}: 590) following a 2 hr incubation at 37 °C. Fold change in metabolic activity was determined from the non-heat shocked controls within each treatment condition.

Isolation of His10-SUMO2 and His10-Ub substrates.

Purification of SUMOylated and ubiquitinated proteins was performed as described previously[58]. In short, cells expressing His10-SUMO2 or His10-Ub were washed three time in ice-cold PBS, and then a small fraction was used as an input control lysed in SNTBS lysis buffer (2% SDS, 1% NP-40, 50 mM Tris pH 7.5, 150 mM NaCl) while the remaining cells were lysed in denaturing lysis buffer containing 6 M guanidine-HCl, 100 mM Na2HPO4/NaH2PO4 and 10 mM TRIS, buffered at pH 8. Lysates were normalized for protein content, supplemented with 10 mM imidazole pH 8 and 5 mM β-mercaptoethanol and subsequently incubated with 20 µl dry volume Ni-NTA agarose beads/ml lysate overnight at 4 °C. Beads were subsequently washed with wash buffers 1 to 4. Wash buffer 1 contained 6M guanidine-HCL, 100 mM Na2HPO4/NaH2PO4, 10 mM Tris pH 8, 10 mM imidazole pH 8, 0.2% Triton X-100 and 5 mM β-mercaptoethanol. Wash buffer 2 contained 8 M urea, 100 mM Na2HPO4/NaH2PO4, 10 mM Tris pH 8, 10 mM imidazole pH 8, 0.2% Triton X-100 and 5 mM β-mercaptoethanol. Wash buffer 3 contained 8 M urea, 100 mM Na2HPO4/NaH2PO4, 10 mM Tris pH 6.3, 10 mM imidazole pH 7, 0.2% Tri-ton X-100 and 5 mM β-mercaptoethanol. Wash buffer 4 contained 8 M urea, 100 mM Na2HPO4/NaH2PO4, 10 mM Tris pH 6.3, 0.1% Triton X-100 and 5 mM β-mercaptoethanol. For purifications which were subsequently analyzed by mass spectrometry, wash buffer 2 contained only 0.1% Triton X-100 and Triton X-100 was left out of wash buffers 3 and 4. Washes were performed for 15 min at room temperature and wash 4 was performed twice. His10-tagged proteins were eluted twice with 7 M urea, 100 mM Na2HPO4/NaH2PO4, 10 mM Tris pH 7 and 500 mM imidazole. For mass spectrometry, elutions were concentrated by using a 100k cut-off filter and diluted with ammonium bicarbonate (ABC) to a concentration of 50 mM. Samples were reduced with dithiothreitol (DTT) and alkylated with cloroacetamide (CAA). Eluted fractions were further diluted with 50 mM ABC to attain a final urea concentra-tion of 2 M.Proteins were digested with sequencing grade trypsin in a 1:50 enzyme-to-protein ratio overnight at 25

°C. Peptides were acidified with 2% trifluoroacedic acid (TFA). The peptide samples were subsequently desalted and concentrated using homemade reversed phase StageTips. For the StageTips, three layers of C18 matrix was gently pushed into filter-less 200µl pipet tips. The matrix was activated by HPLC-grade methanol, subsequently washed twice with 80% acetonitrile (ACN) in 0.1% formic acid (FA) and equilibrated with 0.1% FA. Sample was passed through the StageTip and was subsequently washed twice with 0.1% FA and centrifuged to complete dryness[59]. Peptides were eluted twice from StageTips using 40% acetonitrile (ACN) in 1% formic acid (FA) and 60% ACN in 1% FA, respectively.

Mass Spectrometry Data Collection and Analysis.

Four biological replicates were measured in technical duplicates by nanoflow liquid chromatography-tandem mass spectrometry (nanoLC-MS/MS) on a Q-Exactive Orbitrap (ThermoFisher). Raw data were processed using MaxQuant (1.5.6.0) software. MaxQuant analysis was carried out as previously described[58]. Default settings of MaxQuant software were employed with the following changes, "Label-free quantification (LFQ)" and "Match between runs" were enabled. All settings of MaxQuant parameters can be found via the PRIDE repository and dataset identifier PXD010231. Identified proteins were statistically analyzed using Perseus Software (version 1.5.6). The same experimental conditions of four biological replicates were grouped and LFQ intensities were log2-transformed. Protein groups that were identified in at least three biological replicates in at least one group were selected for further analysis. Missing values were imputed by the software using normally distributed values with a 1.8 (log2) downshift and a 0.3 (log2) width based on total matrix values. Differences in LFQ intensities between groups were analyzed by a two-sample t-test. Proteins were selected based on their fold change and p-value. Protein groups identified in the His10-SUMO2 dn-cHSF1 or GFP cell lines, which did not show a significant change in LFQ intensities (p-value ≤ 0.05) in at least one of the experimental conditions compared to the appropriate parental cell lines, were excluded. Heat shock-responsive SUMOylation of proteins was defined by a ≥ 2-fold increase in abundance post-heat shock compared to no heat shock controls with a p-value ≤ 0.05, in both vehicle and Dox-treated conditions. Proteins that recovered to normal SUMOylation levels post-heat shock were selected based on a ≥ 2-fold decrease 4 hr post-heat shock compared to immediately post-heat shock with a p-value ≤ 0.05. Proteins that retained SUMOylation during heat shock recovery owing to chronic HSF1 inhibition were selected if they showed ≥ 2-fold en-richment in the Dox-treated condition 4 hr post-heat shock condition compared to the vehicle-treated control condition 4 hr post-heat shock with a p-value ≤ 0.05 in addition to no significant difference under the same condition in the inducible GFP cell line. Gene Ontology enrichment analysis was performed on 125 proteins retained during heat shock recovery after chronic HSF1 inhibition using the Gene Ontology Consortium PANTHER Overrepresentation test (release date 2017-12-05) with the annotation version that was released on 2017-11-12.

Cloning, expression and purification of SUMO-MMS21.

PCR amplifications of the cDNA coding region of human MMS21 (Dharmacon OHS1770-202324443) and SUMO3 (Addgene #53143) were cloned into pET-15b vectors containing a 6×-His tag for purification. BL21(DE3) E.coli were transformed with these plasmids, and expression was induced over-night at 16 °C by the addition of isopropyl β-D-1-thiogalactopyranoside (IPTG). Bacteria were lysed by sonication in lysis buffer containing 50 mM Tris, 300 mM NaCl, 10 mM imidazole, 5 mM DTT, 1 mM PMSF, 1 mg/mL lysozyme, 10%

glycerol, at pH 7.8. Recombinant His6-SUMO3-MMS21 and His6-MMS21 were purified by Ni-NTA beads and eluted using 250 mM Imidazole (pH 7.8).

SUMOylation and purification of recombinant FOXM1.
Plasmids containing His6-FoxM1 (pDEST17) and SUMO2+SUMOylation machinery (pT-E1E2S2)[57] were transfected or co-transfected into BL21 E.coli. Expression of proteins was induced overnight at 25 °C by the addition of isopropyl β-D-1-thiogalactopyranoside (IPTG). Bacteria were lysed in 50mM HEPES (pH 7.6), 0.5 M NaCl. 25 mM MgCl2, 50% glycerol, 10% NP-40, 20 mM Imidazole (pH 8), 1 mM PMSF, 1/10ml protease inhibitor cocktail tablets, EDTA-free (SIGMA). Recombinant His6-FoxM1 was purified using TALON metal affinity resin and eluted from beads with 400 mM imidazole (pH 8).

Thermal Shift Analyses.
Recombinant MMS21 or FoxM1 was aliquoted into 11 or 16 samples of 50 µl each and incubated at increasing temperatures from 30–70 °C for 5 min using gradient settings on a Bio-Rad C1000TM Thermal Cycler or a Veriti TM 96-Well Thermal Cycler. For the experiments described in Figure 6C, FoxM1 was aliquoted into samples of 50 µl and incubated for the indicated time periods at the indicated temperatures using a thermo-mixer (Eppendorf). Samples were left to cool down at RT for 3 min then 4 °C for 3 min. 40 µl aliquots were transferred to a micro-centrifuge tube and centrifuged at 20000 x g for 20 min. 25 µl of the soluble fractions were used for immunoblotting analysis.

SENP labelling with activity-based probes (ABPs).
HEK293T-REx cells stably expressing Dox-inducible dn-cHSF1 were treated with Dox for 48 hr prior to heat shock. Cell were exposed to heat shock at 43 °C for 75 min before returning to 37 °C for a 2 hr recovery period. Cells were lysed prior to heat shock, immediately after heat shock, or after 2 hr of recovery. After washing with PBS, cell pellet was split into two. Cell lysates were prepared by resuspending cell pellets in two pellet volumes of lysis buffer (containing 0.25 M sucrose, 20 mM Mops-KOH (pH = 7.4), 1 mM EDTA-NaOH, 1 tablet/10 ml complete mini protease inhibitor cocktail (Sigma), 1 mM DTT) or lysis buffer containing 20 mM N-ethylmaleimide (NEM) and lysed by sonication. After centrifugation (20,000 × g, 4 °C, 5 min), total protein concentration in the supernatant was determined by Bradford. 100 µl of supernatant (~200 µg total protein) was labelled with either 8 µg of Rho-SUMO2-PA or K11 di-SUMO VA ABP for 30 min at 37 °C. The reaction was terminated by the addition of NuPage LDS sample buffer (Invitrogen)[31].

Quantification and statistical analysis
Unless otherwise indicated, experiments were performed in biological triplicate. Results are presented as mean ± standard deviation. Significance for immunobloting quantification was determined using ANOVA analysis followed by post-hoc Tukey analysis (* = $p < 0.05$; *** = $p < 0.0005$). For analysis of data from the mass spectrometry experiments, differences in LFQ intensities between treatment groups were analyzed by a two-sample t-test. Information on biological replicates and statistical significance is included in the figure legends.

Data and software availability
The mass spectrometry proteomics data have been deposited to the ProteomeXchange Consortium via the PRIDE partner repository with the dataset identifier PXD010231.

Supplemental Information

Table S1. Complete list of identified protein groups including statistics, Related to Figure 2
Table S2. List of SUMOylated proteins in response to heat shock, Related to Figure 2
Table S3. List of SUMOylated proteins that recover post-heat shock, Related to Figure 2
Table S4. List of SUMOylated proteins that recover dependent on HSF1 activity, Related to Figure 2

References

1. Kim, Y. E., Hipp, M. S., Bracher, A., Hayer-Hartl, M. and Hartl, F. U. Molecular chaperone functions in protein folding and proteostasis. Annu Rev Biochem 82, 323-355, (2013).
2. Labbadia, J. and Morimoto, R. I. The biology of proteostasis in aging and disease. Annu Rev Biochem 84, 435-464, (2015).
3. Akerfelt, M., Morimoto, R. I. and Sistonen, L. Heat shock factors: integrators of cell stress, development and lifespan. Nat Rev Mol Cell Biol 11, 545-555, (2010).
4. Zou, J., Guo, Y., Guettouche, T., Smith, D. F. and Voellmy, R. Repression of heat shock transcription factor HSF1 activation by HSP90 (HSP90 complex) that forms a stress-sensitive complex with HSF1. Cell 94, 471-480, (1998).
5. Shi, Y., Mosser, D. D. and Morimoto, R. I. Molecular chaperones as HSF1-specific transcriptional repressors. Genes Dev 12, 654-666, (1998).
6. Zhong, M., Orosz, A. and Wu, C. Direct sensing of heat and oxidation by Drosophila heat shock transcription factor. Mol Cell 2, 101-108, (1998).
7. Westerheide, S. D., Anckar, J., Stevens, S. M., Jr., Sistonen, L. and Morimoto, R. I. Stress-inducible regulation of heat shock factor 1 by the deacetylase SIRT1. Science 323, 1063-1066, (2009).
8. Golebiowski, F., Matic, I., Tatham, M. H. et al. System-wide changes to SUMO modifications in response to heat shock. Sci.Signal. 2, ra24, (2009).
9. Tatham, M. H., Matic, I., Mann, M. and Hay, R. T. Comparative proteomic analysis identifies a role for SUMO in protein quality control. Sci.Signal. 4, rs4, (2011).
10. Tempe, D., Piechaczyk, M. and Bossis, G. SUMO under stress. Biochem.Soc.Trans. 36, 874-878, (2008).
11. Guo, C. and Henley, J. M. Wrestling with stress: roles of protein SUMOylation and deSUMOylation in cell stress response. IUbMB Life 66, 71-77, (2014).
12. Sohn, K. C., Lee, K. Y., Park, J. E. and Do, S. I. OGT functions as a catalytic chaperone under heat stress response: a unique defense role of OGT in hyperthermia. Biochem Biophys Res Commun 322, 1045-1051, (2004).
13. Martinez, M. R., Dias, T. B., Natov, P. S. and Zachara, N. E. Stress-induced O-GlcNAcylation: an adaptive process of injured cells. Biochem Soc Trans 45, 237-249, (2017).
14. Marotta, N. P., Lin, Y. H., Lewis, Y. E. et al. O-GlcNAc modification blocks the aggregation and toxicity of the protein alpha-synuclein associated with Parkinson's disease. Nat Chem 7, 913-920, (2015).
15. Hastings, N. B., Wang, X., Song, L. et al. Inhibition of O-GlcNAcase leads to elevation of O-GlcNAc tau and reduction of tauopathy and cerebrospinal fluid tau in rTg4510 mice. Mol Neurodegener 12, 39, (2017).
16. Geiss-Friedlander, R. and Melchior, F. Concepts in sumoylation: a decade on. Nat.Rev.Mol.Cell Biol. 8, 947-956, (2007).
17. Huang, W. C., Ko, T. P., Li, S. S. and Wang, A. H. Crystal structures of the human SUMO-2 protein at 1.6 A and 1.2 A resolution: implication on the functional differences of SUMO proteins. Eur.J.Biochem. 271, 4114-4122, (2004).
18. Flotho, A. and Melchior, F. Sumoylation: a regulatory protein modification in health and disease. Annu.Rev. Biochem. 82, 357-385, (2013).
19. Van der Veen, A. G. and Ploegh, H. L. Ubiquitin-like proteins. Annu.Rev.Biochem. 81, 323-357, (2012).
20. Streich, F. C., Jr. and Lima, C. D. Structural and functional insights to ubiquitin-like protein conjugation. Annu Rev Biophys 43, 357-379, (2014).
21. Saitoh, H. and Hinchey, J. Functional heterogeneity of small ubiquitin-related protein modifiers SUMO-1 versus SUMO-2/3. J.Biol.Chem. 275, 6252-6258, (2000).
22. Hendriks, I. A., D'Souza, R. C., Yang, B. et al. Uncovering global SUMOylation signaling networks in a site-specific manner. Nat Struct Mol Biol 21, 927-936, (2014).
23. Seifert, A., Schofield, P., Barton, G. J. and Hay, R. T. Proteotoxic stress reprograms the chromatin landscape of SUMO modification. Sci Signal 8, rs7, (2015).
24. Martin, N., Schwamborn, K., Schreiber, V. et al. PARP-1 transcriptional activity is regulated by sumoylation upon heat shock. EMBO J. 28, 3534-3548, (2009).
25. Hietakangas, V., Ahlskog, J. K., Jakobsson, A. M. et al. Phosphorylation of serine 303 is a prerequisite for the stress-inducible SUMO modification of heat shock factor 1. Mol. Cell Biol 23, 2953-2968, (2003).

26. Brunet, S. M., De, T. A., Hammann, A. et al. Heat shock protein 27 is involved in SUMO-2/3 modification of heat shock factor 1 and thereby modulates the transcription factor activity. Oncogene 28, 3332-3344, (2009).
27. Seeler, J. S. and Dejean, A. SUMO and the robustness of cancer. Nat Rev Cancer 17, 184-197, (2017).
28. Krumova, P. and Weishaupt, J. H. Sumoylation in neurodegenerative diseases. Cell Mol.Life Sci. 70, 2123-2138, (2013).
29. Moore, C. L., Dewal, M. B., Nekongo, E. E. et al. Transportable, Chemical Genetic Methodology for the Small Molecule-Mediated Inhibition of Heat Shock Factor 1. ACS Chem Biol 11, 200-210, (2016).
30. Schimmel, J., Larsen, K. M., Matic, I. et al. The ubiquitin-proteasome system is a key component of the SUMO-2/3 cycle. Mol.Cell Proteomics 7, 2107-2122, (2008).
31. Mulder, M. P. C., Merkx, R., Witting, K. F. et al. Total Chemical Synthesis of SUMO and SUMO-Based Probes for Profiling the Activity of SUMO-Specific Proteases. Angew Chem Int Ed Engl, (2018).
32. Berkers, C. R., Verdoes, M., Lichtman, E. et al. Activity probe for in vivo profiling of the specificity of proteasome inhibitor bortezomib. Nat Methods 2, 357-362, (2005).
33. Lamoliatte, F., McManus, F. P., Maarifi, G., Chelbi-Alix, M. K. and Thibault, P. Uncovering the SUMOylation and ubiquitylation crosstalk in human cells using sequential peptide immunopurification. Nat Commun 8, 14109, (2017).
34. Cuijpers, S. A. G., Willemstein, E. and Vertegaal, A. C. O. Converging Small Ubiquitin-like Modifier (SUMO) and Ubiquitin Signaling: Improved Methodology Identifies Co-modified Target Proteins. Mol Cell Proteomics 16, 2281-2295, (2017).
35. Malakhov, M. P., Mattern, M. R., Malakhova, O. A. et al. SUMO fusions and SUMO-specific protease for efficient expression and purification of proteins. J.Struct.Funct.Genomics 5, 75-86, (2004).
36. Butt, T. R., Edavettal, S. C., Hall, J. P. and Mattern, M. R. SUMO fusion technology for difficult-to-express proteins. Protein Expr. Purif 43, 1-9, (2005).
37. Henley, J. M., Craig, T. J. and Wilkinson, K. A. Neuronal SUMOylation: mechanisms, physiology, and roles in neuronal dysfunction. Physiol Rev 94, 1249-1285, (2014).
38. Vedadi, M., Niesen, F. H., Allali-Hassani, A. et al. Chemical screening methods to identify ligands that promote protein stability, protein crystallization, and structure determination. Proceedings of the National Academy of Sciences of the United States of America 103, 15835-15840, (2006).
39. Pinton, G. F., Dahl, J., Rosenzweig, S. and Trahey, G. E. A heterogeneous nonlinear attenuating full-wave model of ultrasound. IEEE Trans. Ultrason. Ferroelectr. Freq. Control 56, 474-488, (2009).
40. Zhou, W., Ryan, J. J. and Zhou, H. Global analyses of sumoylated proteins in Saccharomyces cerevisiae. Induction of protein sumoylation by cellular stresses. J. Biol. Chem 279, 32262-32268, (2004).
41. Anckar, J. and Sistonen, L. Regulation of HSF1 function in the heat stress response: implications in aging and disease. Annu Rev Biochem 80, 1089-1115, (2011).
42. Khalil, S., Luciano, J., Chen, W. and Liu, A. Y. Dynamic regulation and involvement of the heat shock transcriptional response in arsenic carcinogenesis. Journal of cellular physiology 207, 562-569, (2006).
43. Marblestone, J. G., Edavettal, S. C., Lim, Y. et al. Comparison of SUMO fusion technology with traditional gene fusion systems: enhanced expression and solubility with SUMO. Protein Sci. 15, 182-189, (2006).
44. Butt, T. R., Edavettal, S. C., Hall, J. P. and Mattern, M. R. SUMO fusion technology for difficult-to-express proteins. Protein Expr.Purif. 43, 1-9, (2005).
45. Helenius, A. and Aebi, M. Roles of N-linked glycans in the endoplasmic reticulum. Annu Rev Biochem 73, 1019-1049, (2004).
46. Hendriks, I. A., Lyon, D., Young, C. et al. Site-specific mapping of the human SUMO proteome reveals co-modification with phosphorylation. Nat Struct Mol Biol 24, 325-336, (2017).
47. Cook, J. and Chock, P. B. Ubiquitin: a review on a ubiquitous biofactor in eukaryotic cells. Biofactors 1, 133-146, (1988).
48. Wilson, V. G. and Heaton, P. R. Ubiquitin proteolytic system: focus on SUMO. Expert.Rev.Proteomics 5, 121-135, (2008).
49. Nagaraj, N. and Mann, M. Quantitative analysis of the intra- and inter-individual variability of the normal urinary proteome. J. Proteome. Res 10, 637-645, (2011).
50. Kim, W., Bennett, E. J., Huttlin, E. L. et al. Systematic and quantitative assessment of the ubiquitin-modified proteome. Mol. Cell 44, 325-340, (2011).

51. Guerrero, C., Tagwerker, C., Kaiser, P. and Huang, L. An integrated mass spectrometry-based proteomic approach: quantitative analysis of tandem affinity-purified in vivo cross-linked protein complexes (QTAX) to decipher the 26 S proteasome-interacting network. Mol.Cell Proteomics. 5, 366-378, (2006).
52. Kopito, R. R. Aggresomes, inclusion bodies and protein aggregation. Trends Cell Biol 10, 524-530, (2000).
53. Balchin, D., Hayer-Hartl, M. and Hartl, F. U. In vivo aspects of protein folding and quality control. Science 353, aac4354, (2016).
54. Jucker, M. and Walker, L. C. Self-propagation of pathogenic protein aggregates in neurodegenerative diseases. Nature 501, 45-51, (2013).
55. Liebelt, F. and Vertegaal, A. C. Ubiquitin-dependent and independent roles of SUMO in proteostasis. Am J Physiol Cell Physiol 311, C284-296, (2016).
56. Flotho, A., Werner, A., Winter, T. et al. Recombinant reconstitution of sumoylation reactions in vitro. Methods Mol.Biol. 832, 93-110, (2012).
57. Uchimura, Y., Nakamura, M., Sugasawa, K., Nakao, M. and Saitoh, H. Overproduction of eukaryotic SUMO-1- and SUMO-2-conjugated proteins in Escherichia coli. Anal.Biochem. 331, 204-206, (2004).
58. Hendriks, I. A. and Vertegaal, A. C. Label-Free Identification and Quantification of SUMO Target Proteins. Methods Mol Biol 1475, 171-193, (2016).
59. Rappsilber, J., Mann, M. and Ishihama, Y. Protocol for micro-purification, enrichment, pre-fractionation and storage of peptides for proteomics using StageTips. Nat.Protoc. 2, 1896-1906, (2007).

Figure S1

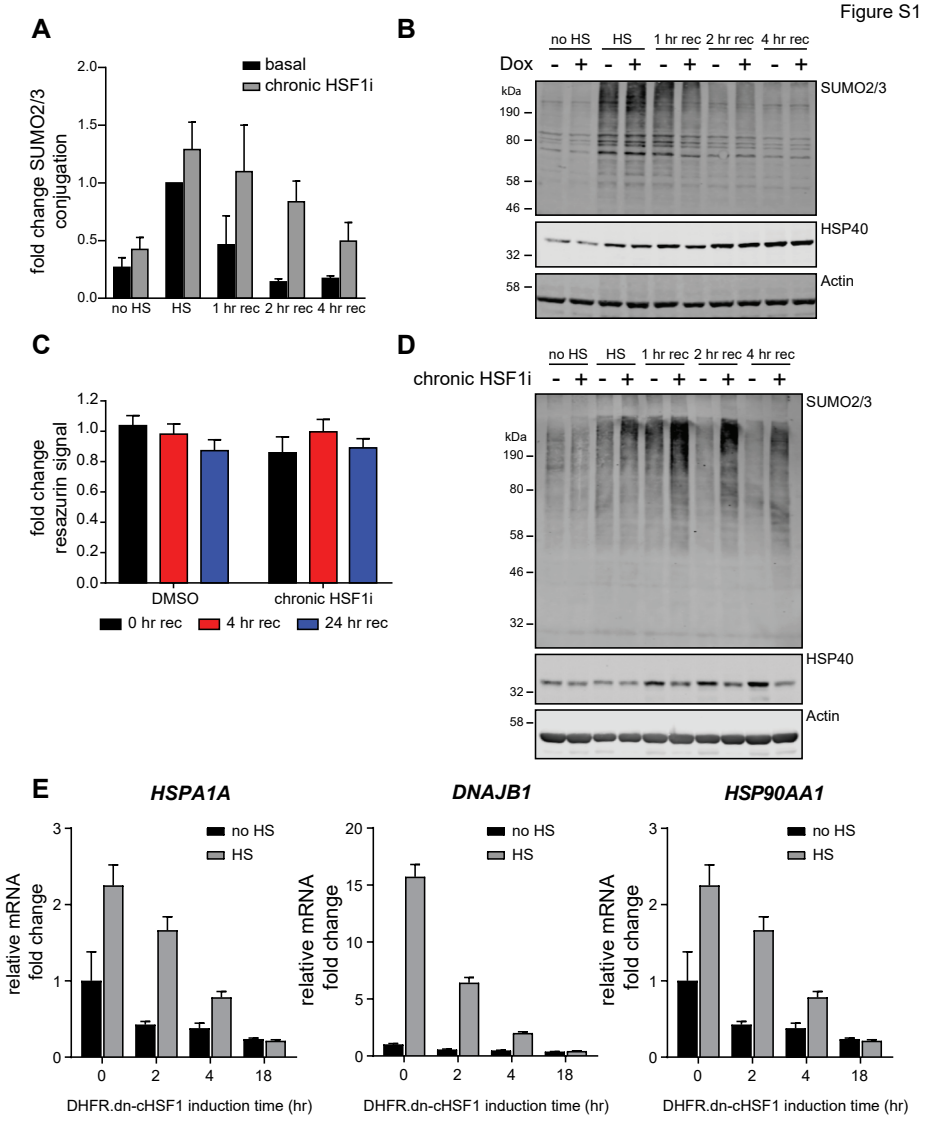

Figure S1. Depletion of proteostasis factors via chronic HSF1 inhibition delays recovery of SUMO2/3 conjugation levels after heat shock. Related to Figure 1. (**A**) Quantification of conjugated SUMO2/3 substrates from Figure 1C. Bar graphs show the fold change in SUMO2/3 conjugation at the specified time points as compared to the vehicle-treated HS sample. Error bars indicate the standard deviation, n = 3. HS, heat shock; rec, heat shock recovery. (**B**) HEK293T-REx cells expressing Dox-inducible GFP were treated with Dox for 48 hr prior to HS. Cells were exposed to HS at 43 °C for 75 min before returning to 37 °C for recovery (rec) and lysed as indicated. Total amounts of SUMOylated proteins were analyzed by immunoblotting. HSP40 levels were used to confirm induction of the heat shock response. β-Actin was used as a loading control. (**C**) HEK293T-REx cells expressing Dox-inducible dn-cHSF1 were treated with Dox for 48 hr prior to HS. Cells were exposed to HS at 43 °C for 75 min before returning to 37 °C for recovery. Analysis of cell viability was performed using the resazurin assay before HS, or at the indicated recovery time points. (**D**) LX2 cells expressing DHFR.dn-cHSF1 were treated with TMP for 48 hr (chronic HSF1i) prior to heat shock (HS). Cells were exposed to HS and lysed at indicated time points. Total amounts of SUMOylated proteins were analyzed by immunoblotting. HSP40 levels were used to confirm induction of the heat shock response and to confirm functional HSF1 inhibition. β-Actin was used as a loading control. (**E**) HEK293T-REx cells expressing DHFR.dn-cHSF1 were treated with either TMP or vehicle for the indicated time points before exposing to a 1-hr HS at 43 °C. Bar graphs show relative fold change of HSPA1A (HSP70.1) and DNAJB1 (HSP40) and HSP90AA1 (HSP90) mRNA analyzed by qRT-PCR.

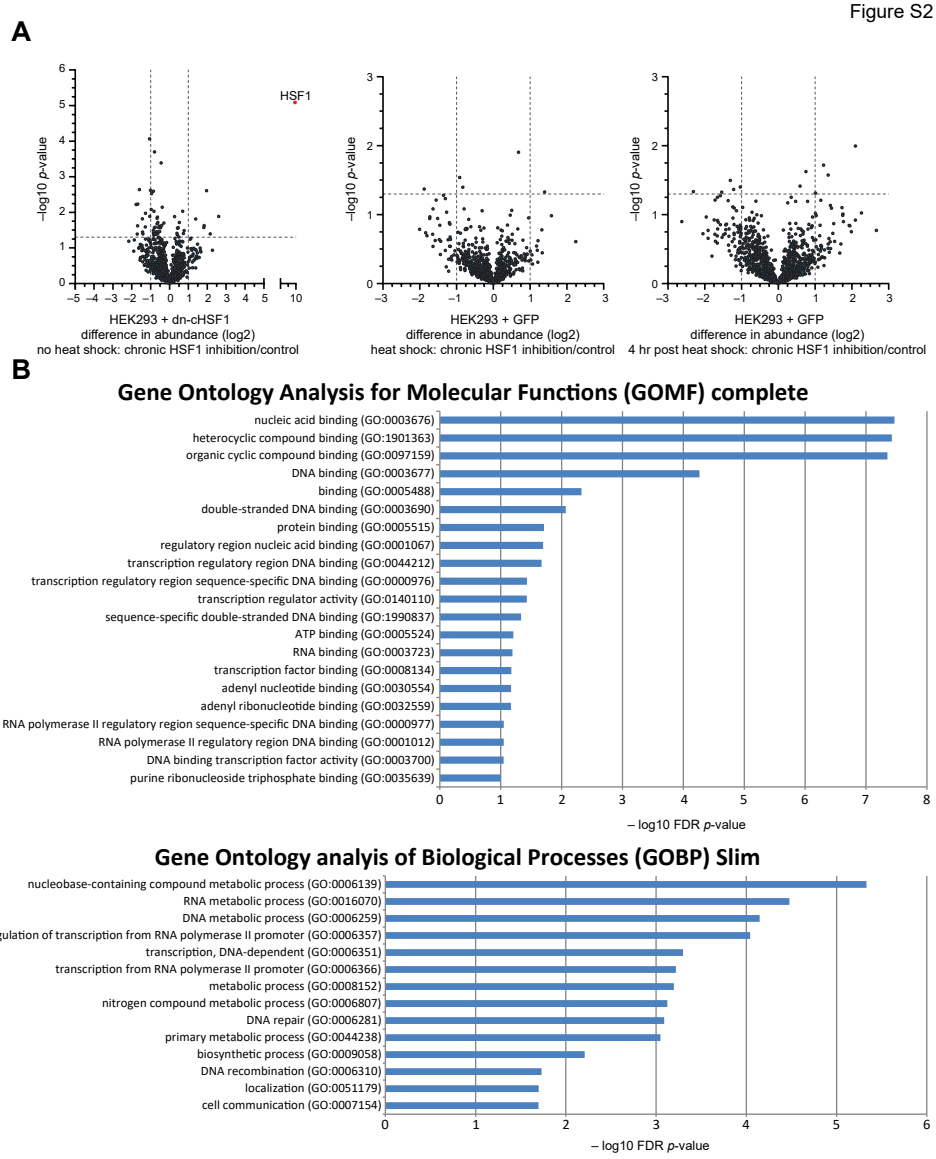

Figure S2. SUMOylation response of control conditions and complete GO analysis of SUMOylated proteins whose recovery after heat shock was delayed by chronic HSF1 inhibition. Related to Figure 2.

(**A**) Volcano plots depicting the statistical differences in abundance between proteins identified by mass spectrometry. Dashed lines indicate a cut-off at a p-value ≤ 0.05 (–log10 p-value = 1.3) and a fold change ≥ 2 (log2 = 1). The left panel shows SUMOylated proteins identified prior to heat shock (HS) in the Dox-inducible dn-cHSF1 cell line specifically in the Dox-treated (chronic HSF1i) sample as compared to the untreated sample. The middle panel shows SUMOylated proteins identified immediately after HS in the Dox-inducible GFP cell line, specifically in the Dox-treated sample as compared to the untreated sample. The right panel shows SUMOylated proteins identified 4 hr post HS in the Dox-inducible GFP cell line, specifically in the Dox-treated sample as compared to the untreated sample. (**B**) Complete gene ontology analysis for molecular functions (GOMF) of proteins whose recovery post-HS was delayed by chronic HSF1 inhibition. Terms with a –log10 False Discovery Rate (FDR) > 2 are shown (upper panel). SLIM biological processes (GOBP) of proteins whose recovery after HS was delayed by chronic HSF1 inhibition. Terms with a –log10FDR of > 1.3 are shown.

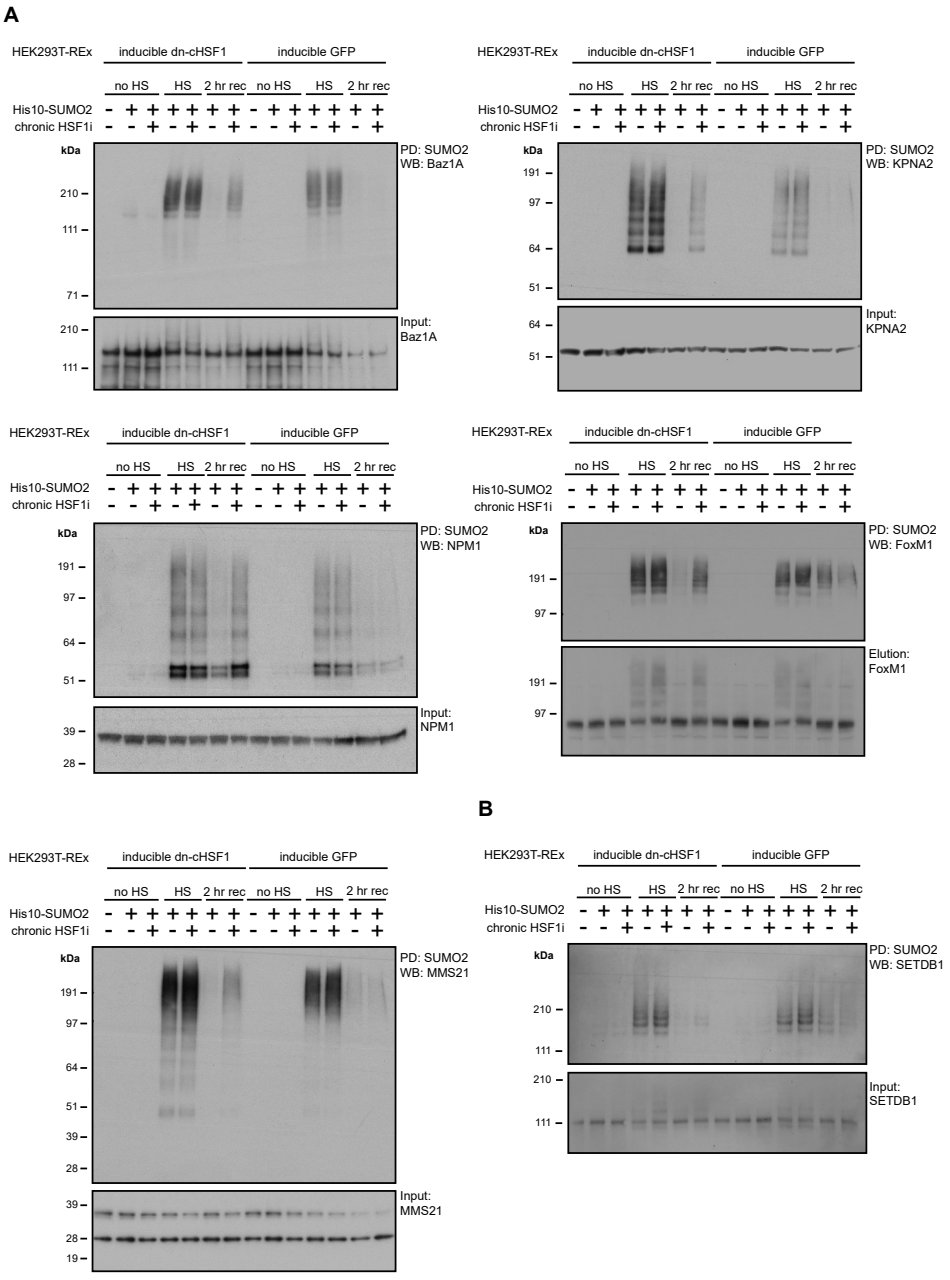

Figure S3. Validation of SUMOylation targets that were identified by proteomics. Related to Figure 2.
(**A**) SUMOylation targets whose recovery after heat shock (HS) was delayed by chronic HSF1 inhibition. HEK293T-REx cells stably co-expressing His10-SUMO2 and Dox-inducible dn-cHSF1 or GFP were treated with Dox for 48 hr (chronic HSF1i) prior to HS. Cells were exposed to HS at 43 °C for 75 min before returning to 37 °C for a 2-hr recovery period (rec) and lysed as indicated. SUMOylated proteins were purified by means of His10-purification. Elutions and inputs were analyzed by immunoblotting for Baz1A (upper left panel), KPNA2 (upper middle panel), MMS21 (upper right panel), NPM1 (lower left panel) and FoxM1 (lower right panel). (**B**) SUMOylation targets whose recovery after HS was not delayed by chronic HSF1 inhibition. HEK293T-REx cells stably co-expressing His10-SUMO2 and Dox-inducible dn-cHSF1 were treated as in (A). Elutions and inputs were analyzed by immunoblotting for SETDB1.

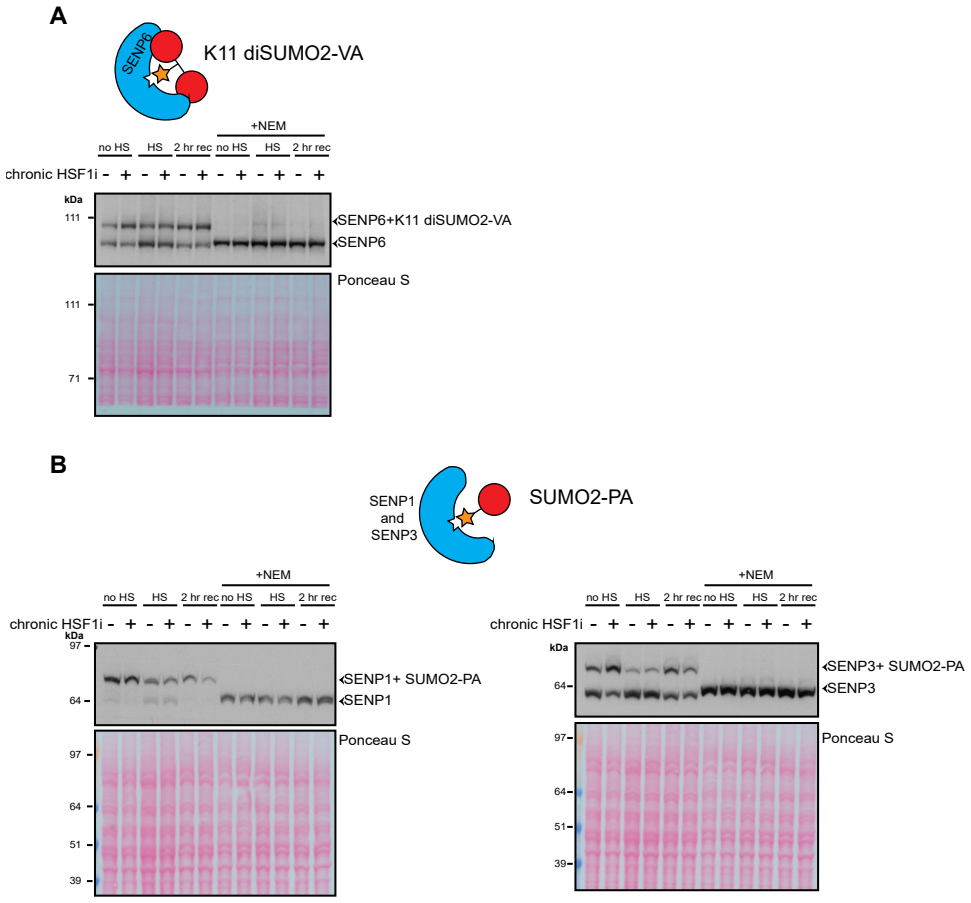

Figure S4. Modulation of the proteostasis network does not alter activity of SENPs. Related to Figure 3. (**A**) Where indicated, HEK293T-REx cells expressing Dox-inducible dn-cHSF1 were treated with Dox for 48 hr (chronic HSF1i) prior to heat shock (HS). Cells were exposed to HS at 43 °C for 75 min before returning to 37 °C for a 2-hr recovery period (rec). Cells were lysed in native lysis buffer with or without N-ethylmaleimide (NEM), a cysteine protease inhibitor which should inhibit activity and therefore labelling of the SENPs. Lysates were incubated with K11 diSUMO2-vinylamide (VA) activity-based probe (ABP) for 30 min at 37 °C. Immunoblot analysis was performed using a specific antibody against SENP6. Active SENPs are covalently labelled with the ABP, which leads to a size shift on the SDS gel. (**B**) HEK293T-REx cells were treated as in (A), labelling of active SENPs was carried out with SUMO2-propargyl (PA) ABP. Immunoblot analysis was performed using specific antibodies against SENP1 (left panel) and SENP3 (right panel).

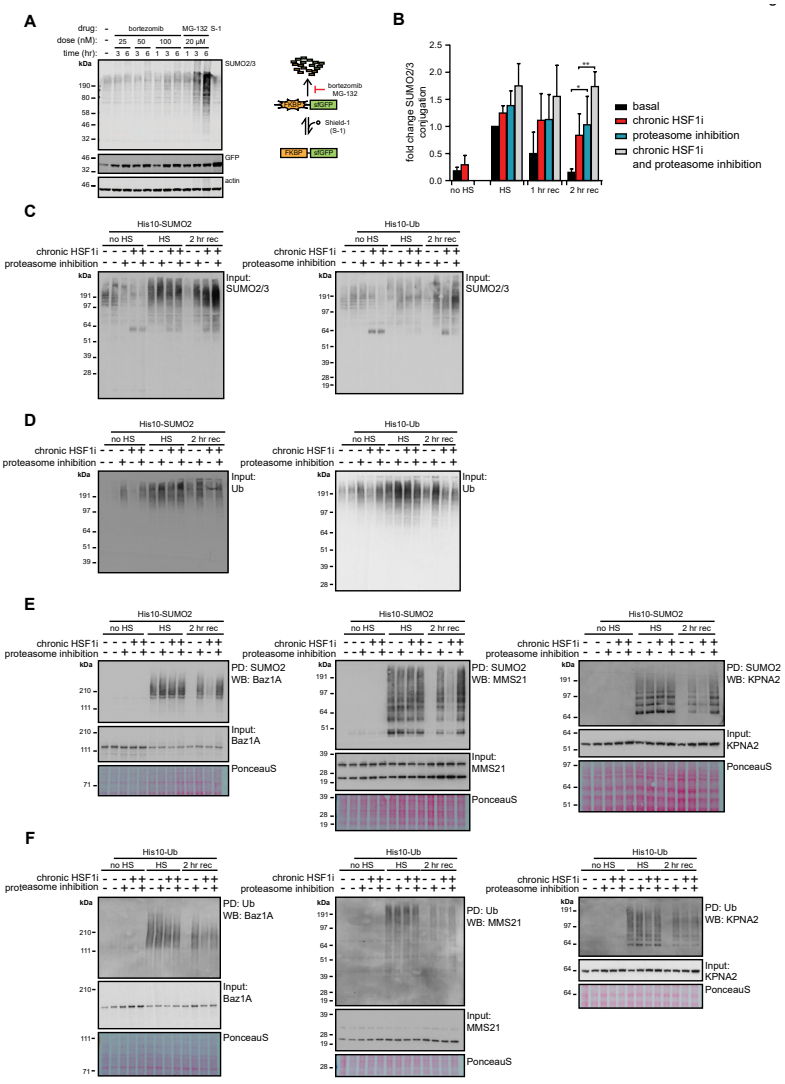

Figure S5. An intact proteostasis network is needed for degradation of SUMO and Ub substrates during heat shock recovery. Related to Figure 3. (**A**) HEK293T-REx cells stably expressing FKBP.sfGFP were treated with up to 100 nM bortezomib or 20 μM MG-132 for up to 6 hr of treatment. Total amounts of SUMOylated proteins were analyzed by immunoblotting. Proteasome inhibition was analyzed by immunoblotting for GFP to confirm stabilization of FKBP-sfGFP. The ligand for FKBP, Shield-1 (S-1), was used as a positive control for FKBP-sfGFP stabilization. (**B**) Quantification of fold change of SUMOylation before, during, and after HS as shown in Figure 3A. n = 3, error bars indicate standard deviations. Significance was determined using ANOVA analysis followed by post-hoc Tukey analysis, * = $p < 0.05$; ** = $p < 0.005$. (**C**) HEK293T-REx cells stably co-expressing His10-SUMO2 or His10-Ub and Dox-inducible dn-cHSF1 were treated with Dox for 48 hr (chronic HSF1i) prior to heat shock (HS), with 100 nM bortezomib (proteasome inhibition) immediately prior to HS, or with a combination of both. Cells were exposed to HS at 43 °C for 75 min before returning to 37 °C for a 2-hr recovery period (rec) and lysed as indicated. Input samples were analyzed by immunoblotting for SUMO2/3. (D) HEK293T-REx cells stably co-expressing His10-SUMO2 or His10-Ub and DOX-inducible dn-cHSF1 were treated as in (C). Input samples were analyzed by immunoblotting for Ub. (**E**) HEK293T-REx cells stably co-expressing His10-SUMO2 and Dox-inducible dn-cHSF1 were treated with Dox for 48 hr (chronic HSF1i) prior to heat shock (HS), with 100 nM bortezomib (proteasome inhibition) immediately prior to HS, or with a combination of both. Cells were treated as in (C). SUMOylated proteins were purified by means of His10-purification. Elutions and inputs were analyzed by immunoblotting for Baz1A (left panel), MMS21 (middle panel) and KPNA2 (right panel). Ponceau S stain was used as a loading control for inputs. (**F**) HEK293T-REx cells stably co-expressing His10-Ub and DOX-inducible dn-cHSF1 were treated as in (C). Ubiquitinated proteins were purified by means of His10-purification. Elutions and inputs were analyzed by immunoblotting for Baz1A (left panel), MMS21 (middle panel) and KPNA2 (right panel). Ponceau S stain was used as a loading control for inputs.

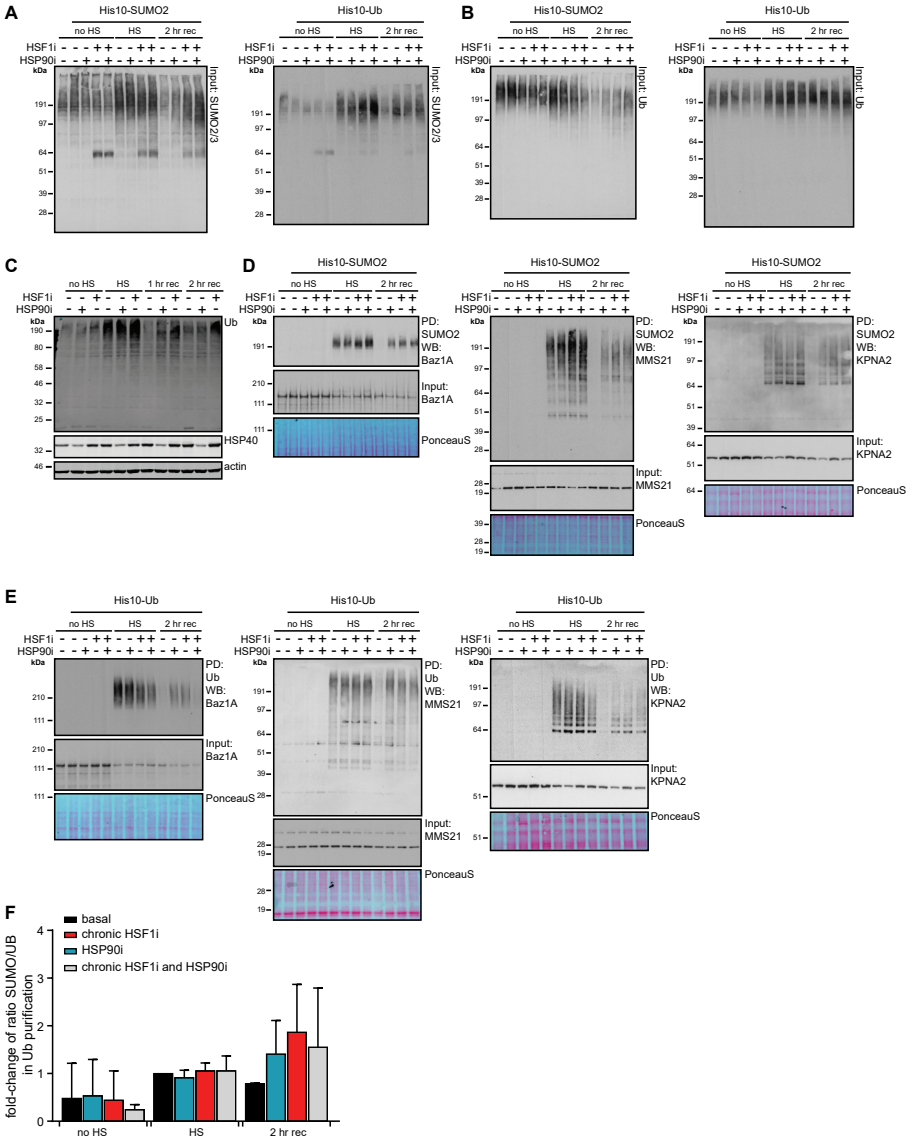

Figure S6. HSP90 plays a key role in the recovery of SUMO2/3 modification to normal levels following heat shock. Related to Figure 5. (**A**) HEK293T-REx cells stably co-expressing His10-SUMO2 or His10-Ub and Dox-inducible dn-cHSF1 were treated with Dox for 48 hr (chronic HSF1i) prior to heat shock (HS), with 500 nM STA-9090 2 hr (HSP90i) prior to HS, or a combination of both. Cells were exposed to HS at 43 °C for 75 min before returning to 37 °C for a 2-hr recovery period (rec) and lysed as indicated. Inputs were analyzed by immunoblotting for SUMO2/3. (**B**) HEK293T-REx cells stably co-expressing His10-SUMO2 or His10-Ub and Dox-inducible dn-cHSF1 were treated as in (A). Inputs were analyzed by immunoblotting for Ub. (**C**) HEK293T-REx cells stably expressing Dox-inducible dn-cHSF1 were treated as in (A). Cells were exposed to HS at 43 °C for 75 min before returning to 37 °C for a recovery period (rec) and lysed as indicated. Total amounts of ubiquitinated proteins were analyzed by immunoblotting. HSP40 levels were used to confirm induction of the heat shock response and to confirm functional HSF1 inhibition. β-Actin was used as a loading control. (**D**) HEK293T-REx cells stably co-expressing His10-SUMO2 and Dox-inducible dn-cHSF1 were treated as in (A). SUMOylated proteins were purified by means of His10-purification. Elutions and inputs were analyzed by immunoblotting for Baz1A (left panel), MMS21 (middle panel) and KPNA2 (right panel). Ponceau S stain was used as a loading control for inputs. (**E**) HEK293T-REx cells stably co-expressing His10-Ub and Dox-inducible dn-cHSF1 were treated as in (A). Ubiquitinated proteins were purified by means of His10-purification. Elutions and inputs were analyzed by immunoblotting for Baz1A (left panel), MMS21 (middle panel) and KPNA2 (right panel). Ponceau S stain was used as a loading control for inputs. (**F**) Bar graph showing the fold-change of the ratio SUMO/Ub within the Ub purified fraction. Error bars represent standard deviation, n = 3.